Gamma-ray decay schemes for ^{93}Kr, ^{93}Rb, and ^{93}Sr†

C. J. Bischof* and W. L. Talbert, Jr.
Ames Laboratory-ERDA and Department of Physics, Iowa State University, Ames, Iowa 50011
(Received 28 June 1976)

The γ rays following the β decays of ^{93}Kr, ^{93}Rb, and ^{93}Sr have been studied, using Ge(Li) detectors for singles and coincidence measurements. A level scheme for ^{93}Y is reported which contains 36 excited levels and 143 of the 162 observed γ rays in the decay of ^{93}Sr. For the decay of ^{93}Rb, 243 γ rays were observed, with 231 placed in a level scheme for ^{93}Sr consisting of 74 excited levels. The decay of ^{93}Kr was observed to have 217 γ rays, 203 of which are placed in a level scheme for ^{93}Rb comprising 56 excited levels. Over 98% of the observed γ-ray intensity is contained in each of the level schemes. Spin and parity assignments are proposed, whenever possible, on the basis of γ-ray transition probabilities and deduced logft values. A comparison is made with available reaction data for the ^{93}Y level scheme, and some of the levels in each decay scheme are interpreted in terms of the nuclear shell model.

[RADIOACTIVITY ^{93}Kr, ^{93}Rb, ^{93}Sr [from ^{235}U(n,f)]; measured E_γ, I_γ, γ-γ coin. Ge(Li) detectors. ^{93}Rb, ^{93}Sr, ^{93}Y deduced levels, J, π, logft. Mass-separated ^{93}Kr activity.]

I. INTRODUCTION

The members of the $A=93$ decay chain are of interest because of their proximity to the subshell and shell closures at $Z=38$ and $N=50$. They are also interesting since they may lie in a transitional region between spherical and deformed nuclei. A report by Talbert and Hanson[1] has already provided a decay scheme for ^{93}Y as well as an interpretation for the levels of ^{93}Zr fed in that decay. Much evidence exists to indicate that nuclei near $A=90$ have a spherical shape. In 1965, Johansson[2] reported the first evidence for deformed nuclei in the $A=100$ mass region. Later, Cheifetz *et al.*[3] presented experimental evidence of the rotationlike behavior of ^{102}Zr and ^{106}Mo. A recent report[4] suggested the onset of deformation in the low-lying excited levels in ^{91}Rb but a later study at this laboratory[5] has contradicted these results.

The decay of ^{93}Sr was first identified by Lieber[6] in 1939. Experimental evidence for the existence of ^{93}Rb was first presented in 1960 by Fritze and Kennett,[7] although its existence had been guaranteed in 1951 when Dillard *et al.*[8] identified its gaseous fission-product parent ^{93}Kr. Previous studies at this laboratory have provided information useful in this work. Carlson *et al.*[9] reported half-lives of 1.289 ± 0.012 sec, 5.86 ± 0.13 sec, and 7.32 ± 0.10 min for the decays of ^{93}Kr, ^{93}Rb, and ^{93}Sr, respectively. Clifford *et al.*[10] have measured Q values for the decays of ^{93}Kr and ^{93}Rb and reported them to be 8.3 ± 0.5 MeV and 7.23 ± 0.10 MeV, respectively. Clifford *et al.* also reported β-decay end-point energies for four β-γ coincidence gates in the decay of ^{93}Kr. However, since no decay scheme existed at the time of Clifford's study, it was not possible to calculate a Q value based on these spectra. By use of the level scheme presented in this work, a weighted average of the decay energies obtained from these gates yields a Q value of 7.51 ± 0.05 MeV. Finally, a Q value of 4.3 ± 0.2 MeV as reported by Bakhru and Mukherjee[11] and by Herzog and Grimm[12] has been adopted for the decay of ^{93}Sr. It should be mentioned that, in the discussion of the ^{93}Y level scheme, evidence will be provided for favoring the upper limit on this Q value.

The first partial level scheme for ^{93}Y based on Ge(Li) detector γ-ray spectra of the decay of ^{93}Sr was proposed by Cavallini, Schussler, and Moussa.[13] In that work, 40 γ rays were identified, of which eight were placed in a level scheme composed of seven levels. These authors were also the first to note the existence of a 759-keV isomeric state. Later, using a similar approach, Herzog and Grimm[12] proposed a level scheme based on 55 transitions between 23 levels. They also assigned spins and parities to the six lowest energy levels based on the ^{94}Zr$(d,{}^3$He) reaction work of Preedom, Newman, and Hiebert.[14] The most recent comprehensive γ study of this decay was performed by Achterberg *et al.*[15] Besides placing 69 transitions within a scheme of 25 levels, they measured the internal conversion coefficients for the 168- and 590-keV transitions as well as a half-life of 85 ± 15 msec for the 759-keV isomeric state. However, their value for the isomer half-life is in great disagreement with a more recent determination of 820 ± 40 msec by Casella, Knight, and Naumann[16] which has been adopted in this work.

No level scheme existed for the decay of ^{93}Rb until the recent concurrent publication of two articles by Achterberg *et al.*[15] and Brissot *et al.*[17] In the former work, the authors provide a level scheme of 20 levels connected by 37 transitions. They also reported the multipolarity of the three lowest-energy γ rays on the basis of measured internal conversion coefficients. Brissot *et al.*, on the other hand, offered a quite different level scheme comprised of 69 transitions placed among 25 levels. There was also little agreement between the γ intensities quoted in these two articles. The γ-ray intensities obtained as a result of the present work should help to resolve this discrepancy.

As in the case of the ^{93}Rb decay, no decay scheme existed for ^{93}Kr prior to the publication of the studies by Achterberg *et al.*[15] and Brissot *et al.*[17] The two level schemes presented for ^{93}Rb are fairly consistent but again there is disagreement in the reported γ-ray intensities. It should be mentioned that Achterberg *et al.* proposed positive parity for the ground state and the first four excited states of the ^{93}Rb level scheme. This parity assignment seems unlikely because of the predominance of negative-parity proton shell-model states available in the region around $Z = 37$. The present study will indicate that the parity of these levels is probably negative in agreement with the predictions of the shell model.

II. EXPERIMENTAL TECHNIQUES

A. Sample preparation

The ^{93}Kr ion beam providing the activity studied in this work was obtained from the thermal neutron fission of ^{235}U. Fission was accomplished by placing a sample of approximately 8 g of uranium stearate in a neutron beam of flux 3×10^9 $n_{\text{th}}/\text{cm}^2/\text{sec}$ provided by the Ames Laboratory Research Reactor. After the gaseous fission products were released they were transferred to the ion source of the TRISTAN on-line isotope separator. The mass-selected ion beam from the isotope separator was then deposited on the aluminum coated Mylar tape of a moving tape collector. The isobaric separation of the resulting activities was then performed by the movement of this tape. Some transitions of nearly equal energies were observed in adjacent decays (e.g., those at 709.95 keV for ^{93}Rb and 710.40 keV for ^{93}Sr decay), which were incompletely separated by tape movement. In those cases, the analyses of the resulting spectra included the contributions resulting from isobaric impurities, figured on the presence and magnitude of obvious impurity transitions. More details on the operation of the TRISTAN on-line mass separator facility are available in Ref. 18.

B. Data accumulation and analysis

Singles and coincidence data were obtained for each nuclide using 60-cm^3 Ge(Li) detectors having an efficiency of approximately 10%. Additional studies were made of the low-energy γ-ray spectrum of ^{93}Kr. Singles and coincidence measurements in that case were also performed using a 1-cm^3 planar detector and one of the 60-cm^3 detectors.

Two Ge(Li) detectors separated by approximately 4 cm were positioned in 180° geometry for all coincidence studies. Events from the two detectors were accepted as being in coincidence if they occurred within a 40 nsec "window." This coincidence information was stored on magnetic tape in the form of pairs of channel numbers corresponding to the two coincidence γ-ray signals. Later a coincidence spectrum was obtained by recording the spectrum defined by the second member of all pairs whose first member corresponds to the gating γ ray of interest.

The relatively low counting rates observed with the $A = 93$ decay chain resulted in difficulties in maintaining equipment stability over a prolonged period of time. Gain shifts occurring due to equipment instability were compensated by frequent recording of accumulated spectra and shifting each singles spectrum before adding to the sum of the previous singles spectra. The program SKEWGAUS[19] was used to determine peak locations and areas as well as their associated errors. These peak locations and areas were converted to energies and intensities on the basis of spectra containing both unknown peaks and γ-ray calibration peaks from ^{56}Co, ^{57}Co, ^{60}Co, ^{182}Ta, and ^{226}Ra. The γ-ray calibration energies used were a weighted average of the values quoted by Greenwood *et al.*,[20-22] Multhauf and Tirsell,[23] and Gunnink *et al.*[24] The detector efficiency curve required for area-to-intensity conversion was based on intensities reported by Gunnink *et al.*,[24] Camp and Meredith,[25] Aubin *et al.*,[26] and Edwards *et al.*[27]

Coincidence spectra for ^{93}Kr, ^{93}Rb, and ^{93}Sr were obtained for 26, 53, and 72 γ-ray gates, respectively. For each gate a second "background" coincidence spectrum was also examined. Peaks having significantly greater areas in the γ-ray gate were considered to be "true" coincidences. These considerations were based either on visual or quantitative inspection.

III. EXPERIMENTAL RESULTS

A. Decay of ^{93}Sr

An enhanced γ-ray spectrum for the ^{93}Sr decay is shown in Fig. 1. Of the 162 photopeaks listed in Table I almost half had not been reported in any previous study of this decay. The multiplets at energies of 167-169, 484-487, 590-594-596, 690-692, 717-718, 1266-1269, 1332-1334, 1978-1981, and 2984-2986 keV had been reported previously to be single γ rays. Coincidence information was used to establish 28 of the 37 levels proposed for the ^{93}Sr decay scheme. A complete tabulation of coincidence relations can be seen in Bischof[28]; they have not been repeated here in the interest of brevity.

144 γ rays, representing more than 99% of the γ-ray intensity observed, are placed in the final level scheme presented in Fig. 2. Coincidence relations have been noted in the level scheme.

Zero ground-state β feeding was adopted for this decay from a study by Bakhru and Mukherjee.[11] This information was used in conjunction with the transition intensity imbalance, corrected for internal conversion (assuming $E3$ multipolarity for the 168.69-keV transition and $M1/E2$ for the other low-energy transitions), to calculate the percent β branching to each level. These calculations result in the absolute transition γ-ray intensities of Fig. 2 and the logft values of Table II.

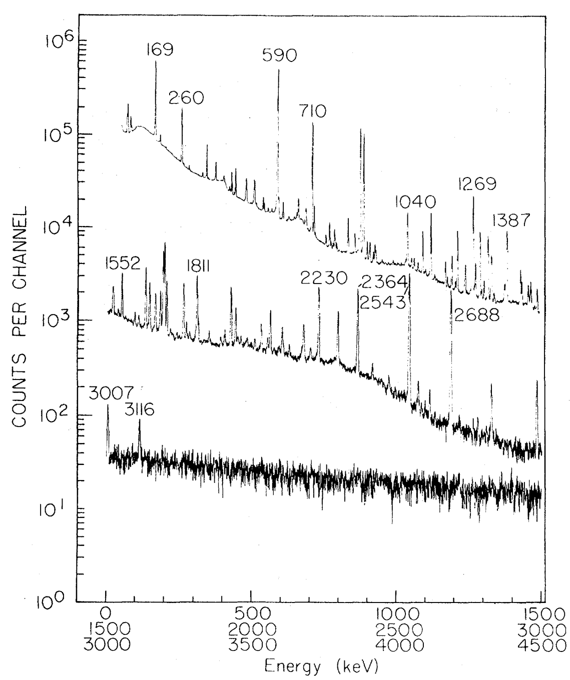

FIG. 1. γ-ray spectrum from the decay of ^{93}Sr.

B. Decay of ^{93}Rb

The enhanced γ-ray spectrum for the ^{93}Rb decay is shown in Fig. 3. Listed in Table III are the 243 photopeaks observed in this decay. Over 50 of the γ rays having a relative intensity greater than 10 have not been reported previously. Included in this tabulation are multiplets at energies of 1148-1150, 1746-1750, 1836-1838-1842, 1992-1998, and 2955-2958 keV which were reported in other works to be single peaks.

The proposed level scheme for ^{93}Sr is shown in Fig. 4, and contains 74 levels based on the placement of 231 γ rays representing approximately 99.5% of the total γ intensity observed. Again coincidence relations have been noted in the level scheme and a complete tabulation is available in Ref. 28.

A ground-state β branching of $(59 \pm 3)\%$ has been adopted from the study of Achterberg *et al.*[15] A branching of $(42 \pm 4)\%$ was reported by Brissot *et al.*,[17] but the absence of any γ spectra in Ref. 17 to illustrate the quality of data presented leads us to hesitate in considering the resulting deduced branching. In this case the absolute intensities and logft values must also be corrected for delayed neutron emission. A delayed neutron probability of $(1.65 \pm 0.30)\%$ from the work of Talbert, Tucker, and Day[29] has been assumed in calculating the logft values in Table IV.

The energies and intensities quoted in this work agree, in most cases, with those provided by Brissot *et al.*,[17] but disagree systematically with those reported by Achterberg *et al.*[15] A comparison of γ-ray intensities for these two works with the present work is presented in Table V. As will be mentioned later, the same type of intensity discrepancy was observed in comparing the results for the ^{93}Kr decay.

The ^{93}Rb decay scheme proposed by Brissot *et al.* is in better agreement with that presented in this work than is that of Achterberg *et al.* In both the levels proposed and the transition energies and intensities, the ^{93}Sr level scheme of Brissot *et al.* appears to be a better skeletal version of that presented here.

C. Decay of ^{93}Kr

The ^{93}Kr enhanced spectrum is provided in Fig. 5. Due to the complexity of the 0–350 keV energy region, a Low Energy Photon Spectrometer (LEPS) spectrum for this region is provided in Fig. 6. The 217 photopeaks of Table VI have all been normalized relative to the 323.9-keV peak, since the most intense peak is actually a multiplet. The total intensity of the 253-keV multiplet quoted elsewhere[15,17] is nearly the same as that reported here

TABLE I. γ-ray transitions observed in the decay of ^{93}Sr.

Energy (keV)	Intensity [a]	Placement	Energy (keV)	Intensity [a]	Placement
166.6 ± 0.3	9.2 ± 2.4	2821–2654	1032.4 ± 0.5	1.5 ± 0.5	2575–1543
168.69 ± 0.05	271 ± 15	759–590	1035.5 ± 0.3	3.0 ± 0.5	1912–876
260.12 ± 0.05	109 ± 6	1136–876	1040.63 ± 0.06	47 ± 3	2688–1647
285.65 ± 0.07	4.0 ± 0.3	876–590	1046.4 ± 0.5	1.4 ± 0.4	3825–2778
332.04 ± 0.07	5.2 ± 0.4	2688–2356	1050.6 ± 0.3	0.50 ± 0.21	3871–2821
342.9 ± 0.4	1.1 ± 0.4	2886–2544	1055.13 ± 0.11	5.1 ± 0.4	2356–1301
346.49 ± 0.05	48.2 ± 2.5	1647–1301	1064.37 ± 0.09	5.5 ± 0.4	2365–1301
377.36 ± 0.06	21.8 ± 1.4	1136–759	1077.86 ± 0.16	3.5 ± 0.4	2356–1278
406.71 ± 0.10	6.3 ± 0.6	1543–1136	1094.00 ± 0.07	25.9 ± 1.5	1853–759
424.70 ± 0.13	3.8 ± 0.5	1301–876	1104.69 ± 0.23	2.2 ± 0.4	1695–590
428.03 ± 0.21	2.2 ± 0.4	2784–2356	1117.1 ± 0.7	1.0 ± 0.4	3895–2778
432.67 ± 0.06	21.8 ± 1.3	1309–876	1122.48 ± 0.06	59 ± 3	2770–1647
440.80 ± 0.18	2.9 ± 0.6	2570–2129	1136.77 ± 0.20	2.9 ± 0.3	2784–1647
446.20 ± 0.06	34.7 ± 1.9	2094–1647	1180.76 ± 0.17	3.6 ± 0.4	2057–876
481.96 ± 0.10	16.7 ± 1.5	2575–2094	1196.23 ± 0.06	14.4 ± 0.8	1787–590
483.73 ± 0.08	24.5 ± 1.8	2575–2091	1200.48 ± 0.74	0.38 ± 0.17	
486.7 ± 0.4	1.8 ± 0.7	2544–2057	1215.48 ± 0.07	36.7 ± 2.0	2091–876
518.50 ± 0.15	1.9 ± 0.3	2575–2057	1239.15 ± 0.25	1.8 ± 0.4	2886–1647
541.89 ± 0.06	10.7 ± 0.6	1301–759	1243.41 ± 0.08	11.8 ± 0.7	2544–1301
545.81 ± 0.07	5.8 ± 0.4	1136–590	1249.2 ± 0.7	1.1 ± 0.4	3825–2575
559.92 ± 0.08	3.0 ± 0.3	1695–1136	1261.3 ± 0.6	1.2 ± 0.5	2570–1309
571.96 ± 0.16	3.1 ± 0.4	3116–2544	1266.38 ± 0.10	16.4 ± 1.2	2575–1309
586.5 ± 0.4	6.6 ± 2.3	2129–1543	1269.47 ± 0.07	105 ± 5	2570–1301
590.28 ± 0.05	1000 ± 55	590–0	1277.99 ± 0.09	12.8 ± 0.9	1278–0
593.81 ± 0.18	16.4 ± 2.1	2688–2094	1308.60 ± 0.09	5.9 ± 0.4	1309–0
596.15 ± 0.13	19.6 ± 2.2	2688–2091	1321.24 ± 0.07	38.4 ± 2.0	1912–590
610.93 ± 0.06	16.0 ± 1.0	1912–1301	1324.8 ± 0.7	0.8 ± 0.3	3895–2570
630.97 ± 0.16	2.9 ± 0.4	2688–2057	1329.6 ± 0.3	1.01 ± 0.20	3116–1787
633.5 ± 0.3	1.6 ± 0.3	1911–1278	1332.5 ± 0.5	7 ± 4	2091–759
650.56 ± 0.15	2.8 ± 0.3	1787–1136	1334.50 ± 0.10	10.0 ± 0.7	2094–759
658.56 ± 0.11	6.2 ± 0.6	2570–1912	1378.98 ± 0.10	5.2 ± 0.4	2688–1309
663.58 ± 0.06	24.2 ± 1.4	2575–1912	1387.11 ± 0.07	51 ± 3	2688–1301
687.79 ± 0.11	9.8 ± 0.9	1278–590	1434.01 ± 0.08	13.3 ± 0.8	2570–1136
690.06 ± 0.12	14.9 ± 1.2	2784–2094	1438.93 ± 0.09	7.4 ± 0.5	2575–1136
692.0 ± 0.4	3.3 ± 0.9	2784–2091	1466.2 ± 0.3	1.5 ± 0.3	2057–590
710.40 ± 0.05	320 ± 17	1301–590	1469.50 ± 0.12	7.7 ± 0.5	2770–1301
716.8 ± 0.5	4.3 ± 2.3	1853–1136	1483.3 ± 0.3	1.5 ± 0.3	2784–1301
718.33 ± 0.12	22 ± 3	1309–590	1492.13 ± 0.12	8.1 ± 0.5	2770–1278
764.8 ± 0.5	0.44 ± 0.17	2821–2057	1506.5 ± 0.6	0.71 ± 0.23	3871–2365
771.19 ± 0.06	17.1 ± 1.0	1647–876	1511.8 ± 0.4	0.81 ± 0.20	2821–1309
776.07 ± 0.13	3.9 ± 0.4	1912–1136	1520.1 ± 0.5	4.7 ± 1.0	2821–1301
782.83 ± 0.15	3.2 ± 0.4	2091–1309	1538.71 ± 0.25	1.5 ± 0.3	2129–590
785.4 ± 0.4	1.1 ± 0.3	2094–1309	1543.4 ± 0.6	0.60 ± 0.22	1543–0
788.68 ± 0.08	11.3 ± 0.7	2575–1787	1551.59 ± 0.09	15.0 ± 0.9	2688–1136
791.10 ± 0.14	3.8 ± 0.4	2091–1301	1609.77 ± 0.20	2.9 ± 0.3	4264–2654
795.29 ± 0.12	3.4 ± 0.3	2886–2091	1634.05 ± 0.08	21.3 ± 1.2	2770–1136
831.3 ± 0.5	0.7 ± 0.3		1642.0 ± 0.6	0.64 ± 0.21	2778–1136
834.89 ± 0.05	24.6 ± 1.3	2688–1853	1647.53 ± 0.08	13.1 ± 0.8	2784–1136
837.85 ± 0.19	1.73 ± 0.24		1652.2 ± 0.7	0.52 ± 0.20	
858.47 ± 0.07	10.7 ± 0.7	2770–1912	1668.7 ± 0.5	2.4 ± 1.3	2544–876
875.73 ± 0.06	360 ± 20	876–0	1684.84 ± 0.13	10.5 ± 0.8	2821–1136
888.13 ± 0.05	325 ± 17	1647–759	1694.07 ± 0.09	38.0 ± 2.1	2570–876
900.98 ± 0.07	10.2 ± 0.6	2688–1787	1699.06 ± 0.09	49 ± 3	2575–876
910.18 ± 0.08	12.1 ± 0.7	1787–876	1706.59 ± 0.10	16.3 ± 1.0	3007–1301
922.70 ± 0.11	4.9 ± 0.4	2570–1647	1742.1 ± 0.4	1.28 ± 0.23	3871–2129
927.69 ± 0.08	9.4 ± 0.7	2575–1647	1765.36 ± 0.09	15.7 ± 0.8	2356–590
930.91 ± 0.10	6.0 ± 0.5	2784–1853	1774.83 ± 0.16	2.4 ± 0.3	2365–590
952.58 ± 0.23	1.6 ± 0.3	1543–590	1786.6 ± 0.3	1.16 ± 0.18	
991.59 ± 0.21	1.8 ± 0.3	2778–1787	1811.45 ± 0.10	20.7 ± 1.2	2688–876

TABLE I. (*Continued*)

Energy (keV)	Intensity [a]	Placement	Energy (keV)	Intensity [a]	Placement
1816.12 ± 0.19	3.4 ± 0.4	2575–759	2203.5 ± 0.7	1.3 ± 0.3	
1894.1 ± 0.3	1.8 ± 0.3	2770–876	2222.0 ± 0.8	0.6 ± 0.3	
1899.46 ± 1.04	0.52 ± 0.19	4264–2365	2230.27 ± 0.12	22.8 ± 1.3	2821–590
1907.73 ± 0.23	2.6 ± 0.3	2784–876	2296.13 ± 0.14	10.9 ± 0.7	2886–590
1928.79 ± 0.10	17.2 ± 1.0	2688–759	2364.72 ± 0.11	23.2 ± 1.3	2365–0
1935.6 ± 0.7	0.50 ± 0.17		2416.3 ± 0.3	1.6 ± 0.3	3007–590
1944.75 ± 0.12	8.2 ± 0.6	2821–876	2472.7 ± 0.3	1.12 ± 0.15	4120–1647
1952.4 ± 0.3	1.46 ± 0.25		2543.84 ± 0.11	44.5 ± 2.4	2544–0
1972.2 ± 0.7	0.49 ± 0.18	3825–1853	2574.2 ± 0.3	1.9 ± 0.3	2575–0
1978.2 ± 0.9	0.39 ± 0.18		2585.9 ± 0.6	0.40 ± 0.12	3895–1309
1981.4 ± 0.8	0.54 ± 0.20	3116–1136	2614.7 ± 0.3	1.32 ± 0.17	
1984.8 ± 0.3	1.20 ± 0.19	2575–590	2688.65 ± 0.12	31.3 ± 1.8	2688–0
2010.80 ± 0.25	1.79 ± 0.25	2886–876	2765.3 ± 0.6	0.61 ± 0.20	
2054.68 ± 0.25	2.0 ± 0.3		2781.6 ± 0.4	0.76 ± 0.11	
2063.64 ± 0.12	9.2 ± 0.6	2654–590	2811.3 ± 0.7	0.31 ± 0.07	4120–1309
2076.6 ± 0.7	0.88 ± 0.24		2828.54 ± 0.20	2.52 ± 0.25	
2094.1 ± 0.6	1.1 ± 0.3		2983.5 ± 0.4	0.66 ± 0.21	4120–1136
2104.78 ± 0.15	4.6 ± 0.4		2985.72 ± 0.21	2.9 ± 0.4	4264–1278
2108.6 ± 0.4	1.30 ± 0.23	3895–1787	2995.7 ± 0.6	0.29 ± 0.07	3871–876
2129.2 ± 0.5	1.5 ± 0.5	2129–0	3006.86 ± 0.22	1.73 ± 0.17	3007–0
2172.0 ± 0.4	1.05 ± 0.19	4264–2091	3116.6 ± 0.4	1.02 ± 0.13	3116–0
2179.49 ± 0.20	4.3 ± 0.6	2770–590			

[a] Relative to I_{590}. Can be converted to I_γ per 100 decays using the factor 0.0665, assuming no β branching to the ground state of ^{93}Y.

but its apportionment is different for each work. The apportionment reported here is based on three independent measurements. Also, the γ ray at 505.8 keV, having an intensity of 34.0 ± 1.8, was determined to be due entirely to sum peaking. In addition, over 40 γ rays with relative intensities greater than 10 have not previously been reported. This number includes multiplets resolved in this work at 643-645, 1059-1061, 1136-1139, 1291-1296, 1711-1713, 1742-1745, 1795-1798, 2557-2561, 2603-2607, and 3227-3230 keV.

The level scheme for the ^{93}Kr decay, presented in Fig. 7, is based on the placement of 203 γ rays among 56 levels. This represents a placement of 98.5% of the observed γ-ray intensity. Coincidence relations have been noted in the level scheme and a complete tabulation is available in Ref. 28.

Zero ground-state β branching tabulation was adopted from the work of Achterberg *et al.*[15] This value, along with a delayed neutron emission probability of (2.6 ± 0.5)%,[29] was used in calculating the absolute intensities and log*ft* values for this decay. The log*ft* values calculated are presented in Table VII.

A comparison of intensities with those reported by Achterberg *et al.* and Brissot *et al.* is made in Table VIII. Again the intensities agree in most cases with those reported by Brissot *et al.* but disagree with those reported by Achterberg *et al.* in the same systematic fashion as for the ^{93}Rb decay. We have been unable to determine the cause for this discrepancy but note that a similar intensity disagreement was reported recently by Glascock, Talbert, and Duke[30] for the decays of ^{91}Kr and ^{91}Rb.

IV. DISCUSSION

An overwhelming majority of the levels above 2.5 MeV in the level schemes for ^{93}Rb, ^{93}Sr, and ^{93}Y proposed in this study have not been reported previously. The inclusion of these levels alters the β feeding percentages for previously reported levels and hence the spin and parity assignments based on deduced log*ft* values. In addition, several new levels below 2.5 MeV have been observed in this study. Spin and parity assignments have been made, whenever possible, on the basis of deduced log*ft* values using the rules proposed by Raman and Gove[31] and observed γ-ray transitions.

Previous studies of these nuclides have either failed to provide discussions of the level structure proposed[17] or have based their discussions on an inaccurate interpretation of their experimental results.[12,15] In essence, there are two major points of conflict between this and other

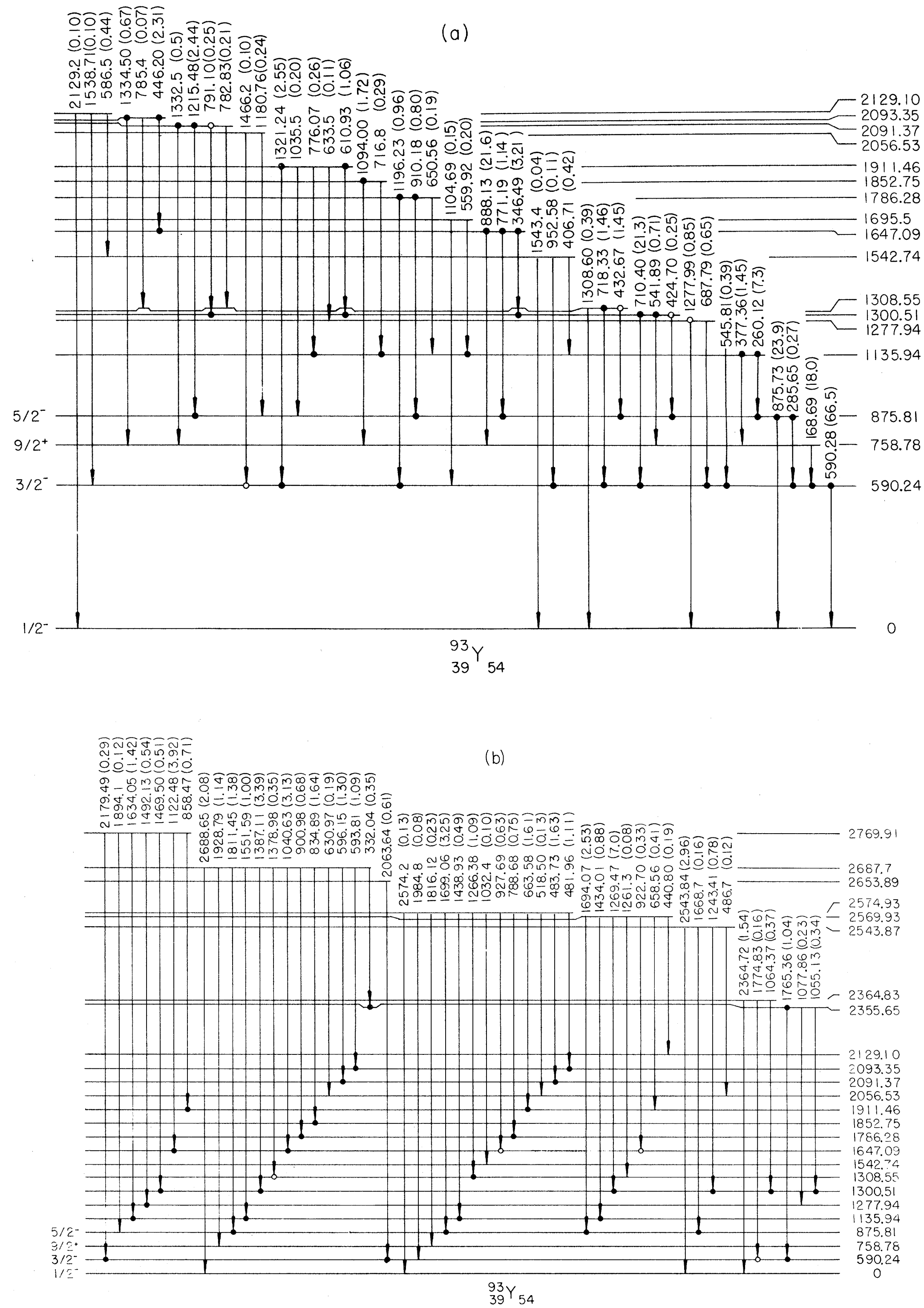

FIG. 2. Level scheme of ^{93}Y populated in the decay of ^{93}Sr. Coincidences are indicated by filled circles at the transition start and termination points (probable coincidences, by open circles). (a) Levels to 2129 keV; (b) levels from 2356 to 2770 keV; (c) levels from 2778 to 4264 keV.

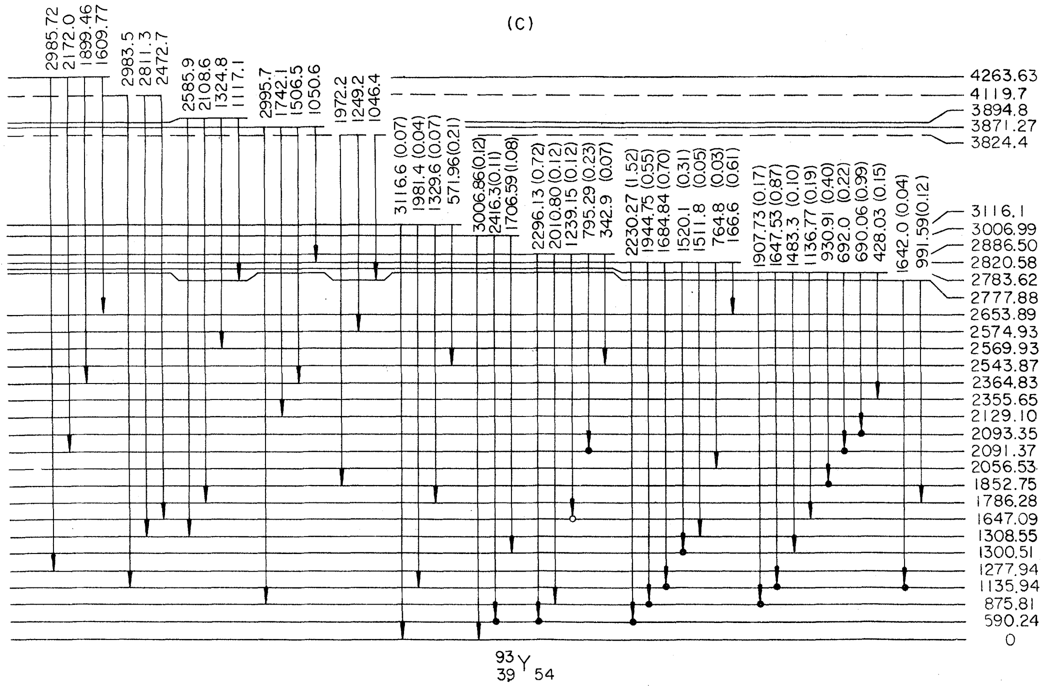

FIG. 2. (*Continued*)

studies. The first point involves the ground state of ^{93}Sr. On the basis of the single-particle model and the systematic trends from ^{89}Sr and ^{91}Sr levels, the expected spin and parity would be $\frac{5}{2}^+$. Such an assignment is proposed by Herzog and Grimm[12] in spite of the fact that the level scheme they provide requires that the $\frac{9}{2}^+$ second-excited state in ^{93}Y be fed in β decay. Some of the other spin and parity assignments of Ref. 12 are then based on this proposal. We will discuss later why we feel the ground state J^π of ^{93}Sr should be $\frac{7}{2}^+$.

The second point of disagreement concerns the ground-state spin and parity for ^{93}Rb. Achterberg *et al.*[15] proposed that the ground state of ^{93}Rb has positive parity on the basis of a deduced log*ft* value of 5.85 ± 0.03 for the ground-state β branch in the decay to ^{93}Sr. This parity is important since Achterberg *et al.* later rely on it as an indication that the ^{93}Rb nucleus is deformed. In view of the expected low-lying shell-model states available for ^{93}Rb, which have negative parity, it is unlikely that the first five excited states in ^{93}Rb would have positive parity. It follows that strict interpretation of the log*ft* value may be unwarranted in this case, especially since that value is in the region where allowed and first forbidden transitions overlap, and a modest reduction of the ground-state β branching would remove the basis for the conclusion (see Sec. III B above for a discussion of β branching on ^{93}Rb decay; in this context, it is unfortunate that Ref. 17 did not present more evidence for their result).

Assuming that ^{88}Sr is an inert core for these nuclides, a description for the level schemes is proposed on the basis of the nuclear shell model. The proton states to be considered are the $2p_{3/2}$, $1f_{5/2}$, and $1f_{7/2}$ hole states and the $2p_{1/2}$ and $1g_{9/2}$ particle states. The $2d_{5/2}$, $3s_{1/2}$, $1g_{7/2}$, and $2d_{3/2}$ states comprise the available neutron states. Experimental evidence exists[32] to indicate that as the mass number increases, the separation between the $2d_{5/2}$ and $1g_{7/2}$ orbits decreases faster than the separation between the $3s_{1/2}$ and $2d_{5/2}$ orbits. This ordering will be important in determining the ground-state spin and parity of ^{93}Sr and ^{93}Kr.

The dominant ground-state configurations for ^{93}Y should be $\pi(2p_{1/2})\nu(2d_{5/2})^4$ and $\pi(2p_{1/2})\nu(1g_{7/2})^4$. In either case, the ground-state spin-parity would be $\frac{1}{2}^-$ in agreement with the results of reaction studies by Preedom *et al.*[14] and Muller.[33] For ^{93}Sr the dominant configurations should be either $(2d_{5/2})^5$ or $(1g_{7/2})^5$. Relatively strong β feeding to the well-established $\frac{9}{2}^+$ level in ^{93}Y indicates the latter configuration is probably appropriate, as suggested earlier.

TABLE II. β branching and logft values for ^{93}Sr decay.

Level energy (keV)	β branching (%)	Logft
0.00	~0 [a]	...
590.24 ± 0.10	~0	...
758.78 ± 0.14	6.6 ± 2.3	7.3 ± 0.2 [b]
875.81 ± 0.10	2.0 ± 1.4	7.8 ± 0.3 [b]
1135.94 ± 0.18	2.5 ± 0.5	7.5 ± 0.1 [b]
1277.94 ± 0.09	0.44 ± 0.10	8.2 ± 0.1 [b]
1300.51 ± 0.10	3.9 ± 1.2	7.2 ± 0.2 [b]
1308.55 ± 0.10	1.41 ± 0.20	7.7 ± 0.1 [b]
1542.74 ± 0.20	~0	...
1647.09 ± 0.16	15.5 ± 1.3	6.4 ± 0.1
1695.5 ± 0.5	0.35 ± 0.02	8.0 ± 0.1 [b]
1786.28 ± 0.22	0.25 ± 0.10	8.1 ± 0.2 [b]
1852.75 ± 0.11	~0	...
1911.46 ± 0.15	1.46 ± 0.20	7.2 ± 0.1 [b]
2056.53 ± 0.25	~0	...
2091.37 ± 0.15	~0	...
2093.35 ± 0.25	~0	...
2129.10 ± 0.13	0.36 ± 0.17	7.7 ± 0.2 [b]
2355.65 ± 0.08	1.13 ± 0.09	7.0 ± 0.1
2364.83 ± 0.14	2.01 ± 0.13	6.7 ± 0.1
2543.87 ± 0.15	3.79 ± 0.24	6.3 ± 0.1
2569.93 ± 0.07	11.5 ± 0.6	5.8 ± 0.1
2574.93 ± 0.20	11.3 ± 0.5	5.8 ± 0.1
2653.89 ± 0.12	~0	...
2687.7 ± 0.4	17.9 ± 0.8	5.5 ± 0.1
2769.91 ± 0.17	7.6 ± 0.4	5.7 ± 0.1
2777.88 ± 0.24	~0	...
2783.62 ± 0.15	3.13 ± 0.17	6.1 ± 0.1
2820.58 ± 0.15	3.8 ± 0.3	6.0 ± 0.1
2886.50 ± 0.17	1.28 ± 0.08	6.4 ± 0.1
3006.99 ± 0.17	1.32 ± 0.09	6.2 ± 0.1
3116.1 ± 0.4	0.38 ± 0.04	6.6 ± 0.2
3824.4 ± 0.4	0.20 ± 0.04	5.4 ± 0.3
3871.27 ± 0.23	0.19 ± 0.03	5.3 ± 0.4
3894.8 ± 0.3	0.23 ± 0.04	5.1 ± 0.4
4119.7 ± 0.3	0.14 ± 0.02	4.2 ± 0.8
4263.63 ± 0.15	0.50 ± 0.04	1.6 ± 3.6

[a] Value adopted from Ref. 11. Q_β of 4.3 ± 0.2 MeV adopted from Refs. 11 and 12.

[b] Logf_1t > 8.5, so cannot exclude first-forbidden unique β transition.

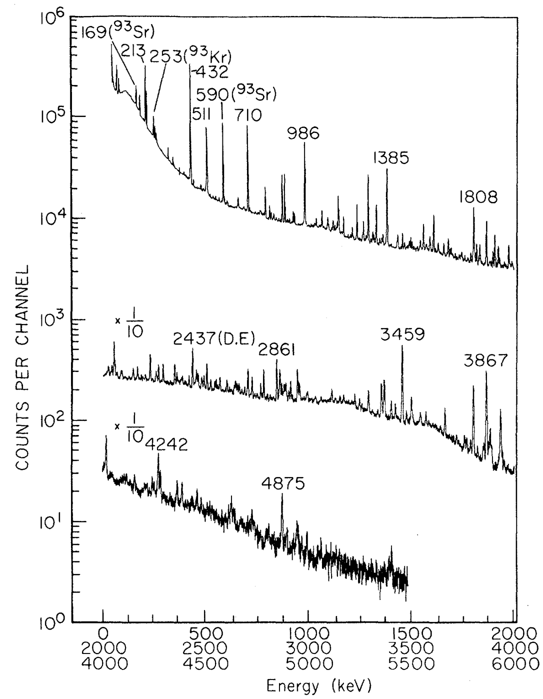

FIG. 3. γ-ray spectrum from the decay of ^{93}Rb.

The possible configurations for the ^{93}Rb ground-state result from the coupling of one of the proton hole states mentioned above to the even neutron configurations. The resulting spin-parity possibilities would be $\frac{3}{2}^-$, $\frac{5}{2}^-$, or $\frac{7}{2}^-$, respectively. Since the assumed $\frac{7}{2}^+$ ground state of ^{93}Sr is β fed in the decay of ^{93}Rb with a logft value of approximately 5.8, the spin must be either $\frac{5}{2}$ or $\frac{7}{2}$. Systematics for the ^{87}Rb, ^{89}Rb, and ^{91}Rb level schemes[32,34,35] indicate that the $\frac{5}{2}$ spin is more likely. In that case the dominant configuration would be $\pi(1f_{5/2})^{-1}\nu(2d_{5/2})^6$ or $\pi(1f_{5/2})^{-1}\nu(1g_{7/2})^6$.

The shell model predicts that the ground-state configuration of ^{93}Kr should be either $\nu[(2d_{5/2})^6$

TABLE III. γ-ray transitions observed in the decay of ^{93}Rb.

Energy (keV)	Intensity [a]	Placement	Energy (keV)	Intensity [a]	Placement
163.40 ± 0.28	6.6 ± 1.5	2456-2293	432.51 ± 0.05	1000 ± 50	433-0
205.21 ± 0.55	6.3 ± 3.2	4714-4509	473.8 ± 0.6	1.6 ± 0.7	4097-3623
213.39 ± 0.05	384 ± 21	213-0	595.87 ± 0.13	12.7 ± 1.7	2869-2273
219.16 ± 0.06	158 ± 9	433-213	602.6 ± 0.4	2.9 ± 0.9	4620-4017
351.74 ± 0.11	3.8 ± 0.4	3955-3603	610.1 ± 0.4	10.1 ± 1.8	3867-3256
404.99 ± 0.18	3.1 ± 0.5		661.64 ± 0.11	16 ± 3	4509-3848

TABLE III. (*Continued*)

Energy (keV)	Intensity [a]	Placement	Energy (keV)	Intensity [a]	Placement
709.95 ± 0.05	308 ± 22	1142–433	1501.18 ± 0.12	20.0 ± 1.3	2886–1385
721.99 ± 0.17	2.9 ± 0.4	3955–3233	1507.77 ± 0.14	13.6 ± 1.1	5385–3877
768.36 ± 0.23	6.6 ± 1.1	1911–1142	1515.8 ± 0.3	5.4 ± 1.0	3867–2351
776.4 ± 0.4	3.0 ± 1.0	3233–2456	1531.1 ± 0.7	3.7 ± 1.1	3804–2273
793.65 ± 0.06	62 ± 3	1780–986	1533.8 ± 0.3	8.1 ± 1.2	5631–4097
822.41 ± 0.22	9.7 ± 1.7	1808–986	1547.78 ± 0.15	16.3 ± 1.3	3867–2319
831.2 ± 0.3	3.6 ± 0.8	4620–3789	1562.91 ± 0.11	58 ± 4	1563–0
859.05 ± 0.18	4.8 ± 0.6	6273–5414	1566.2 ± 0.9	3.4 ± 1.6	1780–213
867.74 ± 0.16	4.2 ± 0.5	3848–2980	1574.71 ± 0.22	7.1 ± 0.8	3867–2293
901.08 ± 0.18	6.3 ± 0.8	2771–1870	1578.0 ± 0.3	8.8 ± 1.2	3623–2045
905.6 ± 0.3	3.8 ± 0.8	2054–1148	1594.61 ± 0.12	33.3 ± 2.1	2980–1385
910.91 ± 0.14	8.2 ± 0.9	4714–3804	1612.87 ± 0.11	96 ± 6	2045–433
929.04 ± 0.09	24.4 ± 1.7	1142–213	1635.20 ± 0.15	21.5 ± 1.8	2621–986
934.70 ± 0.10	18.4 ± 1.4	1148–213	1662.16 ± 0.15	21.0 ± 1.7	3955–2293
981.1 ± 0.3	7.5 ± 1.7	5601–4620	1684.76 ± 0.13	31.6 ± 2.4	2117–433
986.05 ± 0.06	391 ± 20	986–0	1690.9 ± 0.7	3.5 ± 1.2	4042–2351
990.9 ± 0.3	6.5 ± 1.3	2771–1780	1726.3 ± 0.4	4.5 ± 0.9	2869–1142
1035.1 ± 0.5	3.8 ± 1.2	2273–1238	1736.3 ± 1.3	6 ± 3	3877–2141
1054.7 ± 0.3	3.4 ± 0.7	2293–1238	1738.4 ± 0.9	6 ± 4	2886–1148
1059.4 ± 0.3	3.7 ± 0.7	2045–986	1743.2 ± 0.5	6.4 ± 1.8	3789–2045
1068.51 ± 0.11	35 ± 3	3955–2886	1745.7 ± 0.5	6.9 ± 1.8	4097–2351
1077.60 ± 0.17	2.6 ± 0.3	5012–3934	1749.61 ± 0.19	14.5 ± 1.3	3867–2117
1096.71 ± 0.09	23.0 ± 1.4	1529–433	1753.6 ± 0.4	5.4 ± 1.1	5601–3848
1100.63 ± 0.12	10.4 ± 0.9	4991–3891	1793.62 ± 0.18	15.4 ± 1.4	3934–2141
1115.77 ± 0.22	5.4 ± 0.8	3233–2117	1803.6 ± 0.3	13.7 ± 2.0	4577–2774
1120.0 ± 0.4	4.2 ± 1.2	3891–2771	1808.50 ± 0.10	161 ± 8	1808–0
1130.12 ± 0.16	11.0 ± 1.2	2273–1142	1812.76 ± 0.21	14.3 ± 1.6	3198–1385
1138.0 ± 0.3	11.6 ± 1.8	4336–3198	1821.86 ± 0.13	33.0 ± 2.2	3867–2045
1142.58 ± 0.12	18.1 ± 1.5	1142–0	1831.10 ± 0.22	11.9 ± 1.4	3877–2045
1148.18 ± 0.08	88 ± 5	1148–0	1836.4 ± 0.6	16 ± 10	3891–2054
1150.38 ± 0.13	26.7 ± 2.4	2293–1142	1838.0 ± 0.4	27 ± 10	4620–2782
1164.36 ± 0.25	5.2 ± 0.8	3623–2460	1841.6 ± 0.7	4.7 ± 1.4	3404–1563
1167.1 ± 0.5	2.6 ± 0.7	3623–2456	1869.69 ± 0.11	109 ± 6	1870–0
1202.4 ± 0.7	2.7 ± 1.2	4991–3789	1882.9 ± 0.4	5.9 ± 1.2	4620–2737
1204.9 ± 0.7	2.9 ± 1.2	4461–3256	1886.6 ± 0.3	8.3 ± 1.3	2319–433
1208.55 ± 0.19	8.9 ± 1.1	5012–3804	1892.70 ± 0.24	10.0 ± 1.2	3804–1911
1222.7 ± 0.4	4.0 ± 0.9	5012–3789	1900.94 ± 0.12	26.5 ± 1.7	3955–2054
1238.30 ± 0.08	85 ± 5	1238–0	1908.1 ± 0.6	5.6 ± 1.8	5775–3867
1284.0 ± 0.4	8.6 ± 2.0	3603–2319	1910.72 ± 0.12	66 ± 4	1911–0
1287.0 ± 0.5	6.4 ± 2.0	2273–986	1919.0 ± 0.4	6.2 ± 1.2	2351–433
1306.92 ± 0.19	6.6 ± 0.8	2293–986	1927.64 ± 0.12	43 ± 3	2141–213
1315.64 ± 0.10	21.7 ± 1.5	2554–1238	1933.9 ± 0.3	14.8 ± 2.3	3804–1870
1332.97 ± 0.08	61 ± 6	2319–986	1956.4 ± 0.3	10.0 ± 1.3	3867–1911
1349.67 ± 0.21	8.1 ± 1.0	1563–213	1978.28 ± 0.15	46 ± 3	3848–1870
1359.92 ± 0.16	11.8 ± 1.1	6273–4912	1983.2 ± 0.9	4.0 ± 1.8	6000–4017
1365.36 ± 0.11	18.7 ± 1.4	2351–986	1991.8 ± 0.3	9.6 ± 1.3	5396–3404
1385.21 ± 0.08	328 ± 16	1385–0	1997.8 ± 0.6	3.4 ± 1.1	3867–1870
1388.7 ± 0.6	13 ± 3	2774–1385	2023.9 ± 0.4	7.0 ± 1.5	2456–433
1397.7 ± 0.5	3.3 ± 0.9	2782–1385	2026.88 ± 0.25	13.3 ± 1.7	2460–433
1405.37 ± 0.22	5.7 ± 0.7	2554–1148	2037.0 ± 0.8	3.9 ± 1.8	
1437.10 ± 0.16	24.0 ± 2.1	1870–433	2043.82 ± 0.17	17.5 ± 1.4	4912–2869
1439.6 ± 0.5	5.2 ± 1.7	5775–4336	2054.06 ± 0.12	77 ± 4	2054–0
1452.7 ± 0.7	2.9 ± 1.1	3233–1780	2058.78 ± 0.17	20.1 ± 1.7	3867–1808
1470.13 ± 0.22	10.9 ± 1.2	3789–2319	2068.36 ± 0.24	8.2 ± 0.9	3877–1808
1473.2 ± 0.6	3.1 ± 1.0	2460–986	2087.4 ± 0.3	10.0 ± 1.4	3867–1780
1479.1 ± 0.3	3.5 ± 0.7	2621–1142	2147.6 ± 0.3	16.6 ± 2.2	4017–1870
1483.96 ± 0.24	5.0 ± 0.7	4038–2554	2168.24 ± 0.14	25.2 ± 1.8	4038–1870
1491.25 ± 0.24	7.0 ± 1.0	6000–4509	2170.4 ± 1.6	3 ± 3	4790–2621
1494.85 ± 0.15	13.2 ± 1.1	3955–2460	2206.2 ± 0.3	10.4 ± 1.5	6097–3891

TABLE III. (*Continued*)

Energy (keV)	Intensity [a]	Placement	Energy (keV)	Intensity [a]	Placement
2229.44 ± 0.12	54 ± 3	4038-1808	3296.1 ± 1.0	4.0 ± 1.7	5414-2117
2256.2 ± 0.9	4 ± 3	3404-1148	3338.0 ± 0.4	7.8 ± 1.3	5631-2293
2258.4 ± 0.4	15 ± 3	4577-2319	3366.6 ± 0.3	13.0 ± 1.6	4509-1142
2262.0 ± 0.3	8.1 ± 1.1	4042-1780	3370.97 ± 0.16	65 ± 4	3804-433
2270.20 ± 0.12	31.3 ± 1.8	3256-986	3389.8 ± 0.9	3.5 ± 1.1	3603-213
2292.80 ± 0.13	30.7 ± 1.9	2293-0	3403.56 ± 0.18	26.3 ± 1.7	6273-2869
2327.5 ± 0.3	6.6 ± 1.0	3891-1563	3458.19 ± 0.16	214 ± 11	3891-433
2334.0 ± 0.5	3.7 ± 0.8	4790-2456	3477.39 ± 0.24	15.5 ± 1.3	4620-1142
2349.58 ± 0.17	35 ± 3	2782-433	3486.9 ± 0.7	3.9 ± 1.0	6261-2774
2359.45 ± 0.16	18.7 ± 1.3	4912-2554	3501.9 ± 0.4	33 ± 7	3934-433
2377.0 ± 0.3	7.8 ± 1.2	6000-3623	3544.0 ± 0.8	9 ± 3	5414-1870
2386.72 ± 0.23	12.9 ± 1.4	6277-3891	3547.2 ± 0.9	8 ± 3	5601-2054
2398.3 ± 0.3	7.0 ± 1.0	5631-3233	3572.05 ± 0.25	17.1 ± 1.5	4714-1142
2403.5 ± 0.6	3.7 ± 0.9	3789-1385	3585.4 ± 0.5	6.1 ± 1.1	5631-2045
2418.22 ± 0.22	19.1 ± 1.9	3404-986	3642.4 ± 0.6	5.6 ± 1.2	4790-1148
2451.7 ± 0.8	9.3 ± 2.2		3664.75 ± 0.19	31.5 ± 2.1	4097-433
2454.97 ± 0.22	28 ± 3	3603-1148	3706.6 ± 0.7	4.2 ± 1.0	6261-2554
2461.98 ± 0.19	27.6 ± 2.4	3848-1385	3721.6 ± 0.4	8.7 ± 1.4	3934-213
2491.20 ± 0.22	22.6 ± 2.3	3877-1385	3770.4 ± 0.3	10.2 ± 1.2	4912-1142
2505.20 ± 0.15	47 ± 3	3891-1385	3789.3 ± 0.3	8.7 ± 1.1	3789-0
2523.7 ± 0.5	14 ± 5	2737-213	3803.98 ± 0.19	90 ± 5	3804-0
2550.06 ± 0.22	15.4 ± 1.5	4461-1911	3821.9 ± 0.4	5.6 ± 0.8	5385-1563
2557.5 ± 0.4	7.1 ± 1.2	2771-213	3848.7 ± 0.7	6.1 ± 1.4	4991-1142
2568.59 ± 0.20	21.9 ± 1.9	2782-213	3867.60 ± 0.17	148 ± 8	3867-0
2602.38 ± 0.22	20.1 ± 1.9	5385-2782	3876.7 ± 0.3	12.1 ± 1.3	3877-0
2614.1 ± 0.3	7.4 ± 1.1	5385-2771	3883.95 ± 0.22	25.9 ± 1.9	4097-213
2620.2 ± 0.6	4.8 ± 1.1	4912-2293	3890.5 ± 0.3	12.0 ± 1.3	3891-0
2624.8 ± 0.5	5.3 ± 1.1	5396-2771	3934.34 ± 0.18	56 ± 3	3934-0
2638.1 ± 0.4	16.1 ± 2.1	3877-1238	3941.7 ± 0.4	6.5 ± 1.3	6261-2319
2646.6 ± 0.6	10 ± 3	3789-1142	3954.2 ± 1.2	2.2 ± 0.9	3955-0
2652.62 ± 0.22	17.9 ± 1.8	4461-1808	4004.5 ± 0.8	4.5 ± 1.1	6277-2273
2661.08 ± 0.22	17.8 ± 1.7	3804-1142	4009.9 ± 1.2	3.0 ± 1.1	5396-1385
2674.2 ± 0.4	6.1 ± 1.2	6277-3603	4017.55 ± 0.21	23.6 ± 1.7	4017-0
2704.97 ± 0.17	59 ± 4	3848-1142	4156.6 ± 0.6	5.5 ± 1.1	5396-1238
2724.60 ± 0.25	32 ± 5	3867-1142	4242.1 ± 0.5	4.4 ± 0.7	5385-1142
2734.0 ± 1.0	3.4 ± 1.3	3877-1142	4250.9 ± 0.7	2.8 ± 0.7	6707-2456
2766.48 ± 0.17	22.9 ± 1.7	2980-213	4271.23 ± 0.19	19.3 ± 1.3	5414-1142
2773.2 ± 0.4	7.0 ± 1.2	4336-1563	4281.9 ± 0.3	9.7 ± 0.8	4714-433
2799.9 ± 0.4	8.7 ± 1.5	4038-1238	4387.9 ± 0.4	6.7 ± 0.8	6707-2319
2812.6 ± 0.5	6.2 ± 1.4	3955-1142	4461.4 ± 0.4	4.4 ± 0.6	4461-0
2861.34 ± 0.15	64 ± 4	3848-986	4481.2 ± 0.6	3.4 ± 0.6	6261-1780
2869.23 ± 0.18	25.2 ± 1.9	2869-0	4615.4 ± 0.9	2.5 ± 0.8	6000-1385
2875.3 ± 0.6	6.0 ± 1.4	4017-1142	4627.0 ± 0.5	5.9 ± 0.8	5775-1148
2880.48 ± 0.22	21.9 ± 1.8	3867-986	4645.0 ± 0.9	2.5 ± 0.8	5631-986
2886.3 ± 0.3	19.0 ± 2.0	2886-0	4875.1 ± 0.3	10.1 ± 0.8	6261-1385
2890.4 ± 0.3	23.5 ± 2.1	3877-986	4890.0 ± 0.8	1.5 ± 0.3	
2903.6 ± 0.3	12.9 ± 1.5	6707-3804	4899.4 ± 0.5	2.8 ± 0.4	6707-1808
2954.93 ± 0.24	26 ± 3	4097-1142	4947.5 ± 0.6	4.0 ± 0.7	6097-1148
2958.1 ± 0.6	9.3 ± 2.4	5012-2054	4953.9 ± 1.1	2.1 ± 0.5	6097-1142
3027.6 ± 1.1	2.8 ± 1.2	6261-3233	4971.8 ± 0.6	1.9 ± 0.4	
3104.1 ± 0.8	4.1 ± 1.4	4912-1808	4996.8 ± 0.5	2.9 ± 0.5	
3113.85 ± 0.24	21.4 ± 2.0	6000-2886	5138.9 ± 1.0	1.3 ± 0.4	
3129.2 ± 0.8	5.0 ± 1.5		5154.6 ± 1.0	1.3 ± 0.4	
3133.1 ± 0.8	5.1 ± 1.5	4912-1780	5164.8 ± 1.1	1.1 ± 0.4	
3172.1 ± 0.4	11.1 ± 1.5	5631-2460	5396.7 ± 0.9	1.7 ± 0.4	5396-0
3211.6 ± 0.6	6.4 ± 1.3	4991-1780	5409.0 ± 0.7	2.3 ± 0.4	
3226.4 ± 0.3	17.4 ± 1.8	6000-2774			

[a] Relative to I_{432}. Can be converted to I_γ per 100 decays by the factor 0.0125, assuming a ground-state β branch of 59% and a delayed neutron emission probability of 1.65%.

$(1g_{7/2})]$ or $\nu[(1g_{7/2})^6(2d_{5/2})]$. However, the other $N=57$ isotones for which ground-state spin-parity assignments have been made[35,36] are known to have a $\frac{1}{2}^+$ ground state. It also appears that the ground-state spin of ^{95}Sr is less than $\frac{5}{2}$ since feeding to the ground state of ^{95}Y $(\frac{1}{2}^-)$ has been reported.[37] An assignment of $\frac{1}{2}^+$ for the ground state of ^{93}Kr is consistent with the apparent lack of β feeding to the $\frac{5}{2}^-$ ground state of ^{93}Rb while the other values are not. This spin-parity assignment might result from the neutron configuration $\nu[(1g_{7/2})^6(3s_{1/2})]$ or $\nu[(2d_{5/2})^6(3s_{1/2})]$. The shell-model configurations presented above will now be assumed as the ground-state assignments for the $A=93$ nuclei.

A. Levels of ^{93}Y

Most of the spin and parity possibilities proposed for the ^{93}Y levels were based entirely on deduced $\log ft$ values and observed γ transitions. For such levels it is almost impossible to provide a reasonable configuration description. However, the levels at 590, 759, 876, 1136, 1278, 1309, and 3116 keV appear to have been observed also in the reaction studies cited previously. In those cases the number of spin-parity possibilities could be further restricted on the basis of comparison with such reaction data.

An $l_p=1$ distribution was measured for the 590.2-keV level in the ^{94}Zr$(d,{}^3$He) reaction study.[14] Thus

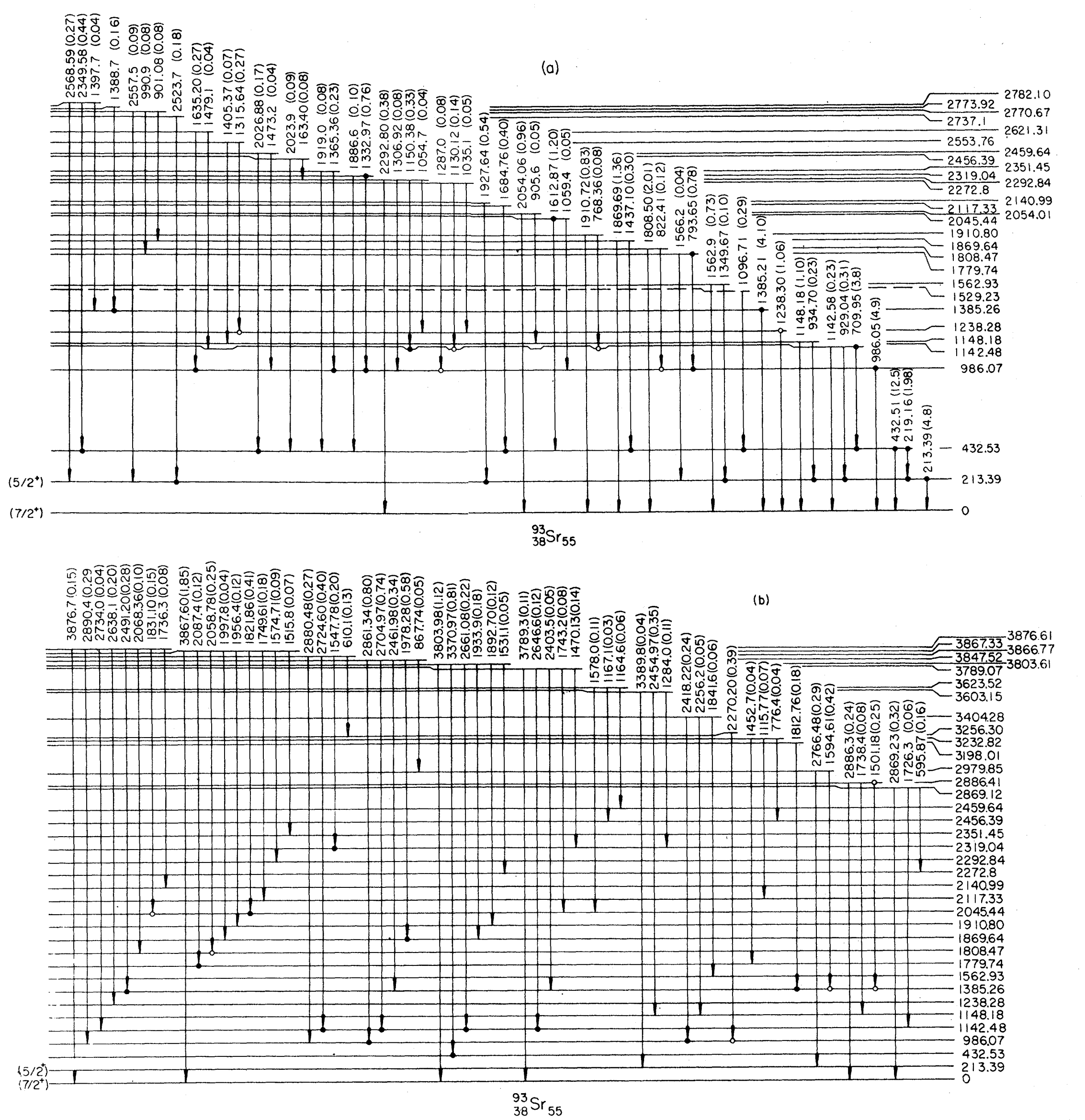

FIG. 4. Level scheme of ^{93}Sr populated in the decay of ^{93}Rb. (a) Levels to 2782 keV; (b) levels from 2869 to 3877 keV; (c) levels from 3891 to 4913 keV; (d) levels from 4991 to 6707 keV.

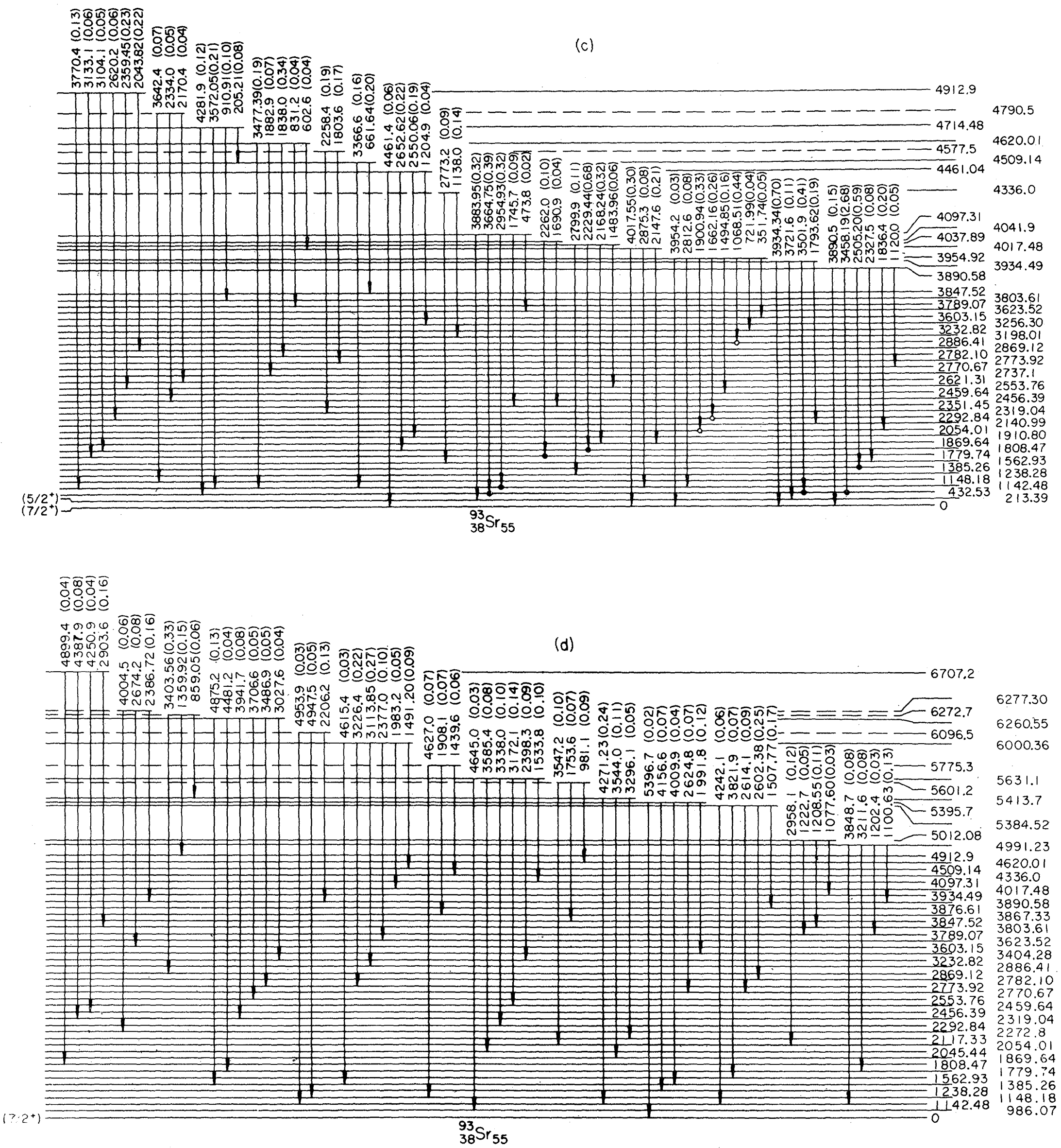

FIG. 4. (Continued)

this state is likely a result of the configuration obtained by coupling a $2p_{3/2}$ proton hole to the lowest-energy coupling of the neutron configuration. The 758.8-keV level was the only $l_p = 4$ transfer detected in Ref. 14. Therefore, it is almost certainly the low-lying $\frac{9}{2}^+$ level predicted by the shell model and previously observed in the level schemes of ^{89}Y and ^{91}Y at approximately the same energy. This state could be explained by the proton configuration $\pi(1g_{9/2})$. The reaction angular distribution for the 875.8-keV level was fitted with an $l_p = 3$ distribution indicating that the dominant configuration is a $1f_{5/2}$ proton hole state. Vervier[38] has calculated that a $\frac{3}{2}^-$, $\frac{5}{2}^-$ doublet should be observed at energies of approximately 0.8 and 1.0 MeV, respectively. These states result from coupling a $2p_{1/2}$ proton to the 2^+ state of the neutron configuration. Configuration mixing between these states and the $\frac{3}{2}^-$ and $\frac{5}{2}^-$ hole states might explain the depressed energy of the latter compared with their energies in the ^{89}Y level scheme. Such mixing would also result in an increased energy for the $\frac{3}{2}^-$ and $\frac{5}{2}^-$ states predicted by Vervier.

Muller[33] measured an $l_p = 3$ distribution for the 1135.9-keV level so that it likely contains a component resulting from a $1f_{7/2}$ proton-hole configu-

TABLE IV. β branching and logft values for ^{93}Rb decay.

Level energy (keV)	β branching (%)	Logft	Level energy (keV)	β branching (%)	Logft
0.00	59±3[a]	5.8±0.1	3603.15±0.12	0.36±0.06	6.7±0.1
213.39±0.06	0.4±0.3	7.9±0.3[b]	3623.52±0.19	0.09±0.03	7.3±0.1[b]
432.53±0.04	1.8±0.7	7.2±0.2[b]	3789.07±0.22	0.36±0.06	6.6±0.1
986.07±0.05	0.5±0.3	7.7±0.3[b]	3803.61±0.18	2.06±0.20	5.9±0.1
1142.48±0.09	2.0±0.3	7.0±0.1[b]	3847.52±0.19	2.14±0.21	5.8±0.1
1148.18±0.11	0.52±0.10	7.6±0.1[b]	3866.77±0.21	0.96±0.11	6.2±0.1
1238.28±0.13	0.30±0.07	7.8±0.1[b]	3867.33±0.20	2.9±0.3	5.7±0.1
1385.26±0.14	1.54±0.25	7.0±0.1[b]	3876.61±0.17	1.07±0.11	6.1±0.1
1529.23±0.10	0.28±0.03	7.7±0.1[b]	3890.58±0.12	3.2±0.3	5.6±0.1
1562.93±0.10	0.50±0.07	7.4±0.1[b]	3934.49±0.17	1.31±0.15	6.0±0.1
1779.74±0.08	0.27±0.06	7.6±0.1[b]	3954.92±0.09	1.33±0.13	6.0±0.1
1808.47±0.11	0.75±0.13	7.2±0.1[b]	4017.48±0.16	0.47±0.06	6.4±0.1
1869.64±0.12	0.14±0.10	7.9±0.3[b]	4037.89±0.11	1.12±0.11	6.0±0.1
1910.80±0.10	0.45±0.07	7.4±0.1[b]	4041.9±0.3	0.14±0.02	6.9±0.1
2045.44±0.10	0.40±0.09	7.4±0.1[b]	4097.31±0.12	1.00±0.10	6.0±0.1
2054.01±0.09	0.26±0.14	7.6±0.2[b]	4336.0±0.3	0.16±0.04	6.7±0.1
2117.33±0.18	0.09±0.04	8.0±0.2[b]	4461.04±0.18	0.49±0.05	6.1±0.1
2140.99±0.12	0.26±0.06	7.5±0.1[b]	4509.14±0.15	0.19±0.06	6.5±0.1
2272.8±0.3	~0	···	4577.5±0.3	0.49±0.06	6.2±0.1
2292.84±0.11	0.23±0.06	7.5±0.1[b]	4620.01±0.15	0.56±0.13	5.9±0.1
2319.04±0.08	~0	···	4714.48±0.14	0.50±0.06	5.9±0.1
2351.45±0.11	0.11±0.04	7.8±0.1[b]	4790.5±0.4	0.15±0.04	6.4±0.1
2456.39±0.19	~0	···	4912.86±0.4	0.58±0.07	5.7±0.1
2459.64±0.42	~0	···	4991.22±0.15	0.31±0.04	5.9±0.1
2553.76±0.19	~0	···	5012.08±0.16	0.30±0.01	5.9±0.1
2621.31±0.15	0.26±0.05	7.3±0.1[b]	5384.52±0.16	0.61±0.06	5.3±0.1
2737.1±0.3	0.10±0.07	7.7±0.3[b]	5395.7±0.5	0.30±0.04	5.6±0.1
2770.67±0.14	0.07±0.03	8.1±0.4[b]	5413.7±0.15	0.32±0.05	5.5±0.1
2773.92±0.22	~0	···	5601.2±0.3	0.25±0.05	5.4±0.1
2782.10±0.20	0.16±0.13	7.5±0.3[b]	5631.1±0.3	0.51±0.06	5.1±0.1
2869.12±0.18	~0	···	5775.3±0.3	0.20±0.04	5.3±0.1
2886.41±0.10	~0	···	6000.36±0.15	0.72±0.08	4.5±0.1
2979.85±0.12	0.62±0.06	6.8±0.1[b]	6096.5±0.5	0.20±0.03	4.9±0.1
3198.01±0.21	0.03±0.03	8.0±0.4[b]	6260.55±0.22	0.37±0.04	4.4±0.1
3232.82±0.14	~0	···	6272.79±0.13	0.51±0.05	4.2±0.1
3256.30±0.13	0.07±0.04	7.1±0.1[b]	6277.30±0.22	0.28±0.04	4.5±0.1
3404.28±0.20	0.22±0.05	7.0±0.1[b]	6707.2±0.3	0.30±0.03	3.5±0.2

[a] Value adopted from Ref. 15. Total of β branching includes delayed neutron emission probability of (1.65±0.30)% from Ref. 29. Q_β of 7.23±0.10 MeV adopted from Ref. 10.

[b] Log$f_1t > 8.5$, so cannot exclude first-forbidden unique β transition.

ration. Preedom *et al.*[14] observe a doublet at 1.28 MeV, while Muller observes the same doublet at an energy of 1.302 MeV. For the $\frac{3}{2}^-$ level, an $l_p = 1$ distribution was observed in both reaction studies while an $l_p = 3$ distribution was observed for the $\frac{5}{2}^-$ level. If the spin-parity assignment is $\frac{3}{2}^-$, the level can be described as containing admixtures of the configurations obtained from coupling a $2p_{1/2}$ proton to the 2^+ state of the even neutron configuration and coupling a $2p_{3/2}$ proton hole to the ground state of the same neutron configuration. The $\frac{5}{2}^-$ level probably contains a large admixture of the configuration resulting from coupling a $1f_{5/2}$ proton-hole state to the ground state of the neutron configuration, while the dominant configuration is the second member of the doublet obtained from coupling a $2p_{1/2}$ proton to the 2^+ state of that same neutron configuration. These configurations probably describe the levels at 1277.9 and 1308.6 keV. The only other level (at 3116 keV) which appears to correspond to the reaction data lies at such a high energy that it is highly speculative to determine the configuration describing it.

TABLE V. Comparison of γ-ray intensities with other ^{93}Rb studies.

Energy (keV)	This work (keV)	Achterberg *et al.* (Ref. 15)	Brissot[a] *et al.* (Ref. 17)
213.39	384 ± 22	385 ± 30	388
219.16	158 ± 9	137 ± 9	152
432.51	1000 ± 50	1000 ± 50	1000
709.95	308 ± 22[b]	250 ± 40	302
793.65	62 ± 3	49 ± 10	66
986.05	391 ± 20	342 ± 30	380
1148.18	88 ± 5	79 ± 5	109
1238.30	85 ± 5	71 ± 7	90
1332.97	61 ± 6	36 ± 5	
1385.21	328 ± 17	80 ± 50	338
1562.91	58 ± 4		62
1612.87	96 ± 6	93 ± 13	104
1808.50	161 ± 8	124 ± 11	152
1869.69	109 ± 6	85 ± 7	110
1910.72	66 ± 4	40 ± 11	74
2054.06	77 ± 4	63 ± 5	75
2229.44	54 ± 3	21 ± 5	55
2704.97	59 ± 4	42 ± 4	58
2861.34	64 ± 4		35
2869.23	64 ± 4		
3370.97	65 ± 4	40 ± 7	80
3458.19	214 ± 11	145 ± 19	255
3803.98	90 ± 5	45 ± 5	107
3867.60	148 ± 8	47 ± 13	174
3934.34	56 ± 3	39 ± 7	54

[a]The intensity uncertainties are reported to vary between 5 and 10% depending on the γ-ray intensity value.

[b]In order to eliminate the contamination resulting from the 710.4-keV γ ray observed in the decay of ^{93}Sr, this intensity has been determined from the 432.5-keV coincidence gate.

Finally, the energy of the level at 1300.5 keV is in excellent agreement with a $\frac{7}{2}^-$ level calculated by Vervier to be at approximately 1.32 MeV. If this assignment is correct the level can be described as resulting from coupling a $2p_{1/2}$ proton to the 4^+ state of the neutron configuration. But in order to account for the β feeding to this level, an admixture of the $\frac{7}{2}^-$ hole state would have to be postulated. It is not obvious from the present study that such an admixture exists.

In Table II it is seen that a log*ft* value of 1.6 is reported for the β feeding of the level at 4264 keV. While this value is unrealistically low, its upper uncertainty limit (due largely to the uncertainty in the Q value) encompasses more reasonable values. It is our conclusion that the Q value is favored to be close to the upper limit (4.5 MeV), rather than near the lower limit as adapted from systematics by Kocher.[39]

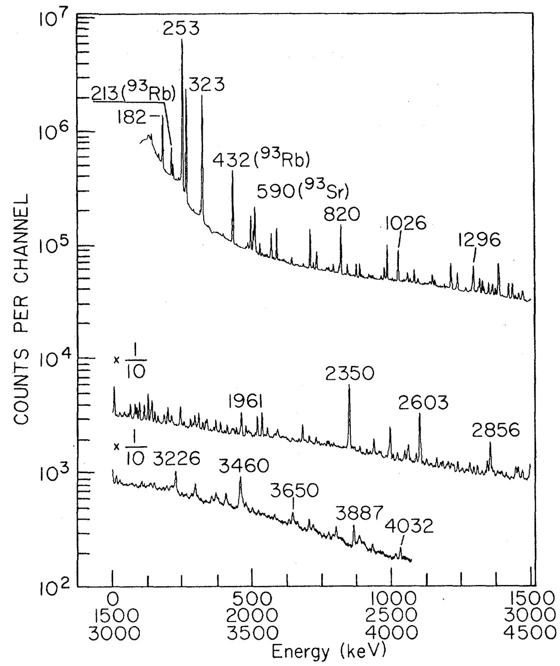

FIG. 5. γ-ray spectrum from the decay of ^{93}Kr.

B. Levels of ^{93}Sr

Since no reaction studies have been made of the levels of ^{93}Sr, the proposed spin-parity possibilities are based only on deduced log*ft* values and observed γ-ray transitions. Furthermore, although Achterberg *et al.*[15] have proposed multipolarities for the 213.4-, 219.2-, and 432.5-keV transitions, these values are suspect because of

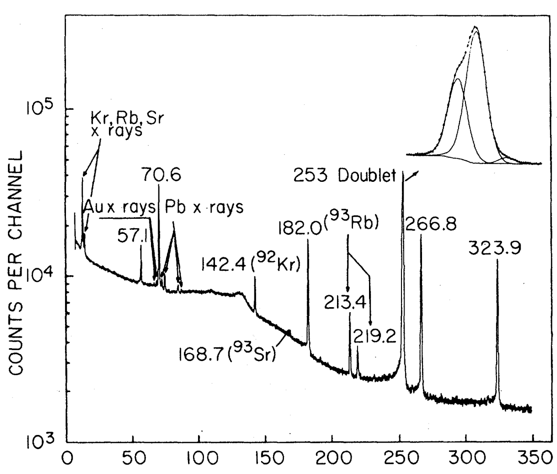

FIG. 6. Low-energy γ-ray spectrum from the decay of ^{93}Kr. The doublet at 253 keV is shown expanded in upper right.

TABLE VI. γ-ray transitions observed in the decay of ^{93}Kr.

Energy (keV)	Intensity [a]	Placement	Energy (keV)	Intensity [a]	Placement
57.11 ± 0.05	10.7 ± 0.05	324–267	1157.09 ± 0.11	13.1 ± 1.0	5237–4080
70.57 ± 0.05	64 ± 3	324–253	1191.49 ± 0.09	9.6 ± 0.6	3801–2609
182.02 ± 0.05	223 ± 12	506–324	1214.98 ± 0.05	73 ± 4	2856–1641
191.06 ± 0.08	3.2 ± 0.3	2856–2665	1235.5 ± 0.3	5.5 ± 0.9	3245–2009
239.26 ± 0.22	6.6 ± 1.2	1880–1641	1238.76 ± 0.06	46.0 ± 2.5	1563–324
252.51 ± 0.06	811 ± 40	506–253	1290.54 ± 0.23	9.9 ± 1.4	1558–267
253.42 ± 0.05	1708 ± 90	253–0	1296.08 ± 0.06	78 ± 4	1563–267
254.83 ± 0.05	29 ± 3	5920–5665	1309.51 ± 0.21	4.3 ± 0.5	1563–253
266.83 ± 0.05	854 ± 40	267–0	1313.44 ± 0.14	12.2 ± 1.0	3002–1689
292.88 ± 0.08	3.75 ± 0.25	1850–1558	1318.38 ± 0.14	38 ± 3	1642–324
316.72 ± 0.09	10.0 ± 0.8	4051–3734	1350.24 ± 0.06	31.0 ± 1.7	1350–0
323.89 ± 0.05	1000 ± 50	324–0	1360.26 ± 0.11	9.4 ± 0.7	3002–1641
399.01 ± 0.12	4.9 ± 0.4	2609–2210	1364.77 ± 0.09	28.3 ± 2.0	1689–324
401.5 ± 0.3	1.9 ± 0.3	1964–1563	1374.78 ± 0.09	17.6 ± 1.2	3063–1689
480.44 ± 0.20	3.6 ± 0.5	2169–1689	1382.7 ± 0.3	7.8 ± 1.6	3551–2169
491.93 ± 0.22	3.3 ± 0.5	3494–3002	1387.92 ± 0.09	56 ± 4	1641–253
496.56 ± 0.05	75 ± 4	820–324	1421.79 ± 0.06	40.0 ± 2.1	1689–267
519.78 ± 0.19	4.0 ± 0.5	3265–2745	1435.35 ± 0.13	42 ± 3	1689–253
529.59 ± 0.05	20.4 ± 1.1	1350–820	1445.64 ± 0.18	8.4 ± 0.9	5496–4051
553.53 ± 0.20	3.2 ± 0.5	820–267	1458.50 ± 0.09	16.4 ± 1.1	1964–506
555.41 ± 0.15	4.3 ± 0.5	3801–3245	1471.3 ± 0.3	15.7 ± 1.7	4080–2609
567.05 ± 0.11	6.9 ± 0.5	820–253	1505.76 ± 0.06	93 ± 5	2856–1350
570.16 ± 0.05	49.4 ± 2.5	2856–2286	1508.41 ± 0.23	9.0 ± 1.3	3359–1850
578.73 ± 0.17	3.5 ± 0.4	6070–5492	1525.89 ± 0.20	8.9 ± 1.0	1850–324
616.51 ± 0.11	4.2 ± 0.3	5665–5049	1528.9 ± 0.3	6.0 ± 0.9	3494–1964
623.64 ± 0.16	2.14 ± 0.23	2265–1641	1543.15 ± 0.11	14.2 ± 1.0	
643.18 ± 0.23	3.8 ± 0.9	2286–1642	1556.32 ± 0.12	10.3 ± 0.8	3245–1689
644.78 ± 0.09	11.2 ± 1.0	2609–1964	1563.09 ± 0.06	39.2 ± 2.1	1563–0
686.51 ± 0.11	5.6 ± 0.4	2856–2169	1576.6 ± 0.6	3.7 ± 1.0	3265–1689
713.3 ± 0.4	2.3 ± 0.4		1586.89 ± 0.07	35.1 ± 2.0	3551–1964
716.9 ± 0.5	2.1 ± 0.5		1596.20 ± 0.06	57 ± 3	1850–253
722.68 ± 0.08	11.3 ± 0.7	2286–1563	1613.33 ± 0.08	14.3 ± 2.5	1880–267
733.72 ± 0.05	36.4 ± 1.9	2084–1350	1616.9 ± 0.8	2.8 ± 1.0	4861–3245
737.24 ± 0.23	2.2 ± 0.3	1558–820	1627.10 ± 0.06	82 ± 4	1880–253
770.7 ± 0.4	5.7 ± 1.0	4051–3280	1638.04 ± 0.19	20.9 ± 1.9	3280–1642
777.57 ± 0.10	8.3 ± 0.6	3063–2286	1641.08 ± 0.06	60 ± 3	1641–0
820.45 ± 0.05	154 ± 8	820–0	1651.87 ± 0.08	28.7 ± 1.7	3002–1350
844.12 ± 0.06	23.3 ± 1.2	1350–506	1662.74 ± 0.13	17.0 ± 1.3	2169–506
852.66 ± 0.12	3.9 ± 0.3	3063–2210	1666.3 ± 0.6	3.4 ± 0.9	3308–1642
891.5 ± 0.6	1.3 ± 0.4	2856–1964	1681.9 ± 0.7	4.0 ± 1.0	3245–1563
895.05 ± 0.13	7.2 ± 0.6	2745–1850	1685.07 ± 0.20	22.7 ± 2.0	2009–324
898.0 ± 0.5	1.8 ± 0.4	5759–4861	1687.4 ± 0.5	6.0 ± 2.0	3245–1558
921.19 ± 0.10	9.4 ± 0.7	3777–2856	1697.84 ± 0.06	58 ± 3	1964–267
965.01 ± 0.11	9.0 ± 0.7	2815–1850	1704.45 ± 0.18	10.5 ± 1.0	2210–506
976.08 ± 0.06	29.4 ± 1.6	2665–1689	1710.78 ± 0.18	20.8 ± 2.2	1964–253
1000.5 ± 0.3	1.9 ± 0.4	3265–2265	1713.4 ± 0.3	12.8 ± 2.0	3063–1350
1005.65 ± 0.09	6.8 ± 0.5	2856–1850	1742.49 ± 0.08	53 ± 3	2009–267
1026.19 ± 0.05	90 ± 5	1350–324	1745.28 ± 0.20	17.2 ± 1.8	3308–1563
1046.57 ± 0.14	5.0 ± 0.5	2609–1563	1755.88 ± 0.19	13.1 ± 1.3	2009–253
1051.7 ± 0.3	3.1 ± 0.5	1558–506	1779.68 ± 0.08	23.8 ± 1.4	2285–506
1054.55 ± 0.23	4.4 ± 0.5	3265–2210	1785.8 ± 0.4	5.1 ± 1.0	4051–2265
1058.71 ± 0.17	12.8 ± 1.7	5920–4861	1788.96 ± 0.17	13.0 ± 1.2	2609–820
1060.53 ± 0.13	15.9 ± 1.8	4861–3801	1794.80 ± 0.08	36.0 ± 2.0	4080–2286
1080.6 ± 0.7	1.7 ± 0.6	6572–5492	1798.3 ± 0.3	7.5 ± 1.0	4861–3063
1083.42 ± 0.06	33.8 ± 1.8	1350–267	1803.71 ± 0.17	9.2 ± 0.8	5049–3245
1097.14 ± 0.09	5.3 ± 1.0	1350–253	1822.3 ± 1.2	7 ± 6	3465–1642
1126.3 ± 0.3	2.8 ± 0.5	2815–1689	1823.8 ± 0.8	14 ± 6	3465–1641
1136.1 ± 0.3	3.2 ± 0.6	1642–506	1840.1 ± 0.3	11 ± 3	4051–2210
1139.17 ± 0.18	8.0 ± 0.7	3308–2169	1850.1 ± 0.3	4.0 ± 0.6	1850–0

TABLE VI. (*Continued*)

Energy (keV)	Intensity[a]	Placement
1862.68 ±0.12	11.0 ±0.8	3551-1689
1886.79 ±0.08	29.0 ±1.7	2210-324
1929.7 ±0.3	13.2 ±2.0	3280-1350
1943.54 ±0.11	19.7 ±1.3	2210-267
1957.10 ±0.18	14.5 ±1.4	2210-253
1961.83 ±0.06	74 ±4	2286-324
1989.3 ±0.3	11.7 ±1.4	3631-1642
1994.41 ±0.21	10.8 ±1.1	2815-820
2011.68 ±0.19	9.5 ±0.9	2265-253
2018.87 ±0.07	58 ±3	2286-267
2035.26 ±0.07	75 ±4	2856-820
2082.62 ±0.14	12.3 ±0.9	5860-3777
2088.24 ±0.19	11.3 ±1.0	3777-1689
2160.0 ±0.5	2.8 ±0.6	3801-1641
2179.3 ±1.2	4 ±3	6260-4080
2181.54 ±0.12	48 ±4	3002-820
2235.4 ±0.8	3.0 ±0.9	5237-3002
2239.2 ±0.3	7.4 ±1.0	2745-506
2308.3 ±0.5	3.1 ±0.7	5860-3551
2342.4 ±0.8	7.3 ±2.5	2609-267
2349.96 ±0.10	306 ±16	2856-506
2366.0 ±0.6	5.3 ±2.0	5860-3494
2368.5 ±0.6	5.7 ±2.0	5920-3551
2411.44 ±0.15	12.8 ±0.9	2665-253
2424.26 ±0.25	7.2 ±0.8	3245-820
2491.2 ±0.3	19 ±3	2815-324
2496.05 ±0.10	95 ±5	3002-506
2517.4 ±0.6	3.2 ±0.7	4080-1563
2521.47 ±0.16	19.6 ±1.2	6572-4051
2531.9 ±0.3	5.4 ±0.6	2856-324
2548.02 ±0.17	25.8 ±2.0	2815-267
2557.26 ±0.16	24.3 ±1.7	3063-506
2561.33 ±0.12	41.4 ±2.4	2815-253
2589.18 ±0.15	21.2 ±1.4	2856-267
2602.61 ±0.11	174 ±9	2856-253
2606.65 ±0.19	29.5 ±2.4	5965-3359
2663.49 ±0.20	21.2 ±2.2	5665-3002
2678.0 ±0.4	10.9 ±1.9	3002-324
2700.5 ±0.3	9.1 ±1.1	4051-1350
2720.2 ±0.4	8.3 ±1.0	5965-3245
2739.14 ±0.12	21.1 ±1.2	3063-324
2755.62 ±0.25	8.9 ±0.9	
2772.9 ±0.3	8.5 ±0.9	
2782.26 ±0.20	22.9 ±1.8	
2796.56 ±0.16	15.0 ±1.0	3063-267
2809.92 ±0.12	18.3 ±1.0	3063-253
2826.62 ±0.24	8.1 ±0.8	5492-2665
2838.5 ±0.3	7.5 ±0.9	5049-2210
2846.0 ±0.5	27 ±12	
2852.6 ±0.5	7.9 ±1.8	3359-506
2855.95 ±0.11	90 ±5	2856-0
2913.5 ±0.3	8.6 ±1.0	3734-820
2944.6 ±0.4	7.3 ±1.2	5759-2815
2948.32 ±0.19	25.1 ±1.7	6725-3777
2956.68 ±0.16	24.8 ±1.7	3777-820
2972.22 ±0.20	18.1 ±1.8	
2998.5 ±0.3	26 ±6	3265-267
3000.5 ±0.5	14 ±6	5665-2665
3014.7 ±0.5	13 ±4	5759-2745
3026.5 ±0.3	7.2 ±1.0	3280-253
3097.7 ±0.5	3.2 ±0.8	
3105.40 ±0.20	12.2 ±1.0	3359-253
3150.8 ±0.5	8.7 ±2.1	5965-2815
3196.8 ±0.7	6.0 ±1.9	6260-3063
3214.5 ±0.3	8.9 ±0.9	6070-2856
3220.3 ±0.3	7.4 ±0.8	4861-1641
3226.70 ±0.15	41 ±3	3494-267
3229.9 ±0.7	6.1 ±2.0	4051-820
3250.3 ±0.3	6.5 ±0.7	5860-2609
3260.7 ±0.5	3.6 ±0.6	6725-3465
3281.1 ±0.7	3.3 ±0.8	5492-2210
3285.3 ±0.3	7.3 ±0.8	5496-2210
3294.8 ±0.8	8.6 ±1.5	3801-506
3298.31 ±0.19	26.6 ±2.1	3551-253
3303.9 ±0.8	4.4 ±1.3	4861-1558
3307.2 ±0.7	4.2 ±1.4	3631-324
3356.0 ±0.5	9 ±3	5965-2609
3358.8 ±1.0	5.0 ±2.5	3359-0
3379.7 ±0.4	7.0 ±1.0	5665-2286
3408.09 ±0.22	18.9 ±1.4	5492-2084
3412.7 ±0.5	5.8 ±1.0	5496-2084
3445.1 ±0.6	2.7 ±0.5	6260-2815
3453.3 ±0.3	8.4 ±1.0	3777-324
3460.7 ±0.6	29 ±5	6725-3265
3464.4 ±1.2	13 ±4	3465-0
3467.2 ±1.0	11 ±5	3734-267
3471.3 ±0.5	6.3 ±1.4	
3482.4 ±0.5	4.9 ±0.8	5492-2009
3582.7 ±0.3	6.3 ±0.6	
3634.7 ±0.3	7.9 ±0.9	5920-2286
3645.9 ±0.5	9.7 ±2.2	5496-1850
3649.2 ±0.4	12.7 ±2.2	5860-2210
3655.5 ±0.5	5.7 ±0.9	5920-2265
3705.87 ±0.16	12.3 ±0.8	
3776.0 ±0.3	6.1 ±0.7	5860-2084
3795.8 ±1.1	1.6 ±0.5	5965-2169
3887.1 ±0.4	5.3 ±0.8	5237-1350
4014.1 ±1.1	2.5 ±1.0	
4032.88 ±0.20	8.8 ±0.7	

[a] Relative to I_{323}. Can be converted to I_γ per 100 decays using the factor 0.0246, assuming no β branching to the ground state of ^{93}Rb and a delayed neutron emission probability of 2.6%.

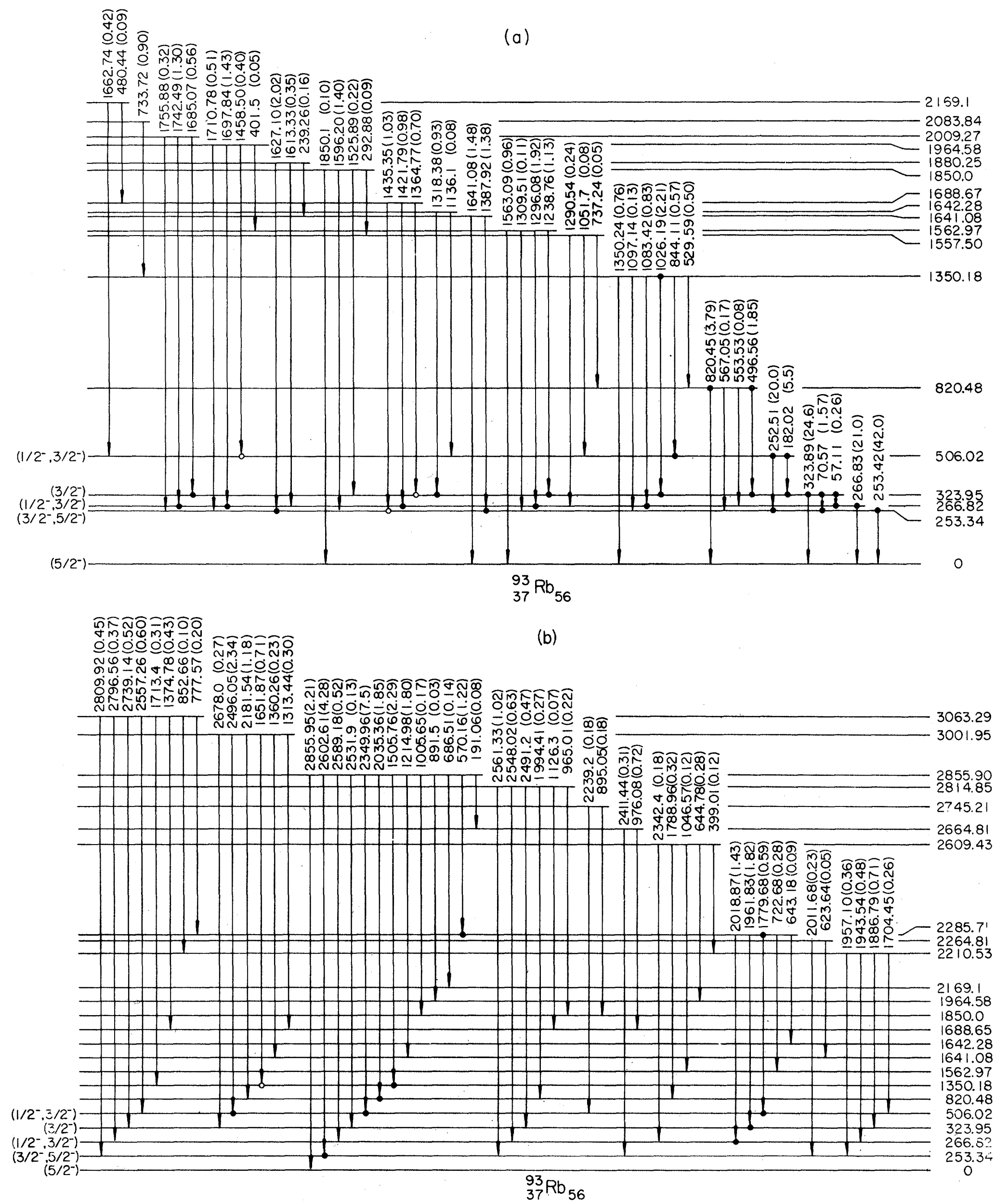

FIG. 7. Level scheme of ^{93}Rb populated in the decay of ^{93}Kr. (a) Levels to 2169 keV; (b) levels from 2211 to 3063 keV; (c) levels from 3245 to 4081 keV; (d) levels from 4861 to 6725 keV.

the change in parity which is then postulated. If the 219.2- and 432.5-keV transitions are both $E1$ the level at 432.5 keV must have negative parity. Such a level cannot be explained by the spherical potential shell model and is inconsistent with the predominance of positive-parity states in this energy region in other odd-A Sr isotopes. In an earlier study[4] Achterberg *et al*. reported a positive-parity state in the level scheme of ^{91}Rb based also on an $E1$ multipolarity transition which Wohn *et al*.[5] subsequently established to have an $M1$ multipolarity. As a result of these complications, spin and parity assignments will be proposed without making use of the suggested $E1$ multipolarity of these 219.2- and 432.5-keV transitions.

Using the reported[15] $E2$ plus $M1$ character (which

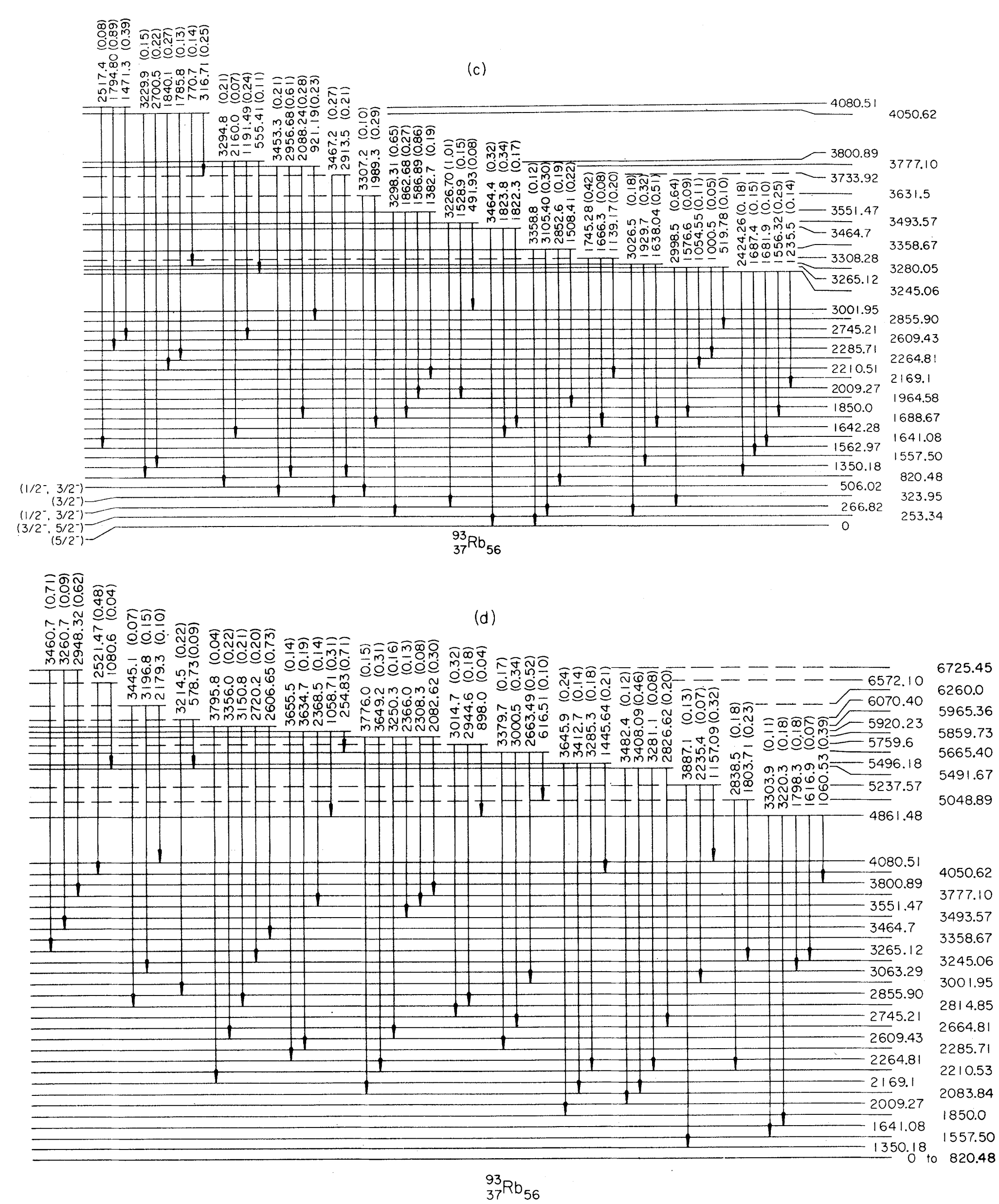

FIG. 7. (*Continued.*)

is reasonable from systematics) of the 213.4-keV transition depopulating the level at that energy, it is possible to limit the spin-parity values to $\frac{5}{2}^+$, $\frac{7}{2}^+$, $\frac{9}{2}^+$. This level is also fed in β decay with a $\log ft$ value of 7.9 which is consistent with these spin-parity values. Since the $2d_{5/2}$ and $1g_{7/2}$ orbits appear to be very close in energy, the spin-parity assignment $\frac{5}{2}^+$ is favored, as arising from a neutron single-particle excitation.

Only the ground state (and, possibly, the 213.4-keV state) can be limited reasonably to a single spin-parity value. As a result, no definitive statements can be made concerning the spin-parity assignments for the other levels of ^{93}Sr. The levels with spin-parity possibilities $\frac{3}{2}^{\pm}$, $\frac{5}{2}^{\pm}$, $\frac{7}{2}^{\pm}$ were fed in β decay with $\log f_1 t$ values less than 8.5 but in addition were depopulated by a ground-state transition. Those levels fed in β decay with $\log ft$ values less than 5.9 could be limited to the spin possibilities $\frac{3}{2}$, $\frac{5}{2}$, $\frac{7}{2}$ with negative parity. If a ground-state transition is observed to depopulate such a level the spin is further restricted to $\frac{5}{2}$, $\frac{7}{2}$.

TABLE VII. β branching and logft values for ^{93}Kr decay.

Level energy (keV)	β branching (%)	Logft	Level energy (keV)	β branching (%)	Logft
0.00	~0 [a]	···	3245.06 ± 0.23	0.20 ± 0.08	6.6 ± 0.2
253.34 ± 0.14	3.0 ± 2.5	6.5 ± 0.4 [b]	3265.12 ± 0.15	0.26 ± 0.20	6.5 ± 0.3
266.82 ± 0.06	7.2 ± 1.1	6.1 ± 0.1	3280.05 ± 0.21	0.86 ± 0.08	6.0 ± 0.1
323.95 ± 0.09	12.9 ± 1.4	5.8 ± 0.1	3308.28 ± 0.18	0.69 ± 0.06	6.1 ± 0.1
506.02 ± 0.08	12.6 ± 1.2	5.8 ± 0.1	3358.67 ± 0.15	0.11 ± 0.10	6.8 ± 0.4 [b]
820.48 ± 0.07	0.6 ± 0.3	7.0 ± 0.2 [b]	3464.7 ± 0.4	0.7 ± 0.4	6.0 ± 0.2
1350.18 ± 0.09	~0	···	3493.57 ± 0.14	1.09 ± 0.09	5.8 ± 0.1
1557.50 ± 0.23	~0	···	3551.47 ± 0.13	1.73 ± 0.11	5.5 ± 0.1
1562.97 ± 0.13	3.02 ± 0.16	6.1 ± 0.1	3631.5 ± 0.3	0.38 ± 0.05	6.2 ± 0.1
1641.08 ± 0.14	~0	···	3733.92 ± 0.12	0.23 ± 0.13	6.3 ± 0.2
1642.28 ± 0.18	~0		3777.10 ± 0.08	0.40 ± 0.07	6.1 ± 0.1
1688.67 ± 0.09	0.19 ± 0.12	7.2 ± 0.3 [b]	3800.89 ± 0.15	0.23 ± 0.06	6.3 ± 0.1
1850.0 ± 0.3	0.76 ± 0.10	6.6 ± 0.1 [b]	4050.62 ± 0.10	0.46 ± 0.11	5.9 ± 0.1
1880.25 ± 0.14	2.49 ± 0.14	6.1 ± 0.1	4080.51 ± 0.08	0.91 ± 0.11	5.5 ± 0.1
1964.58 ± 0.13	1.06 ± 0.12	6.4 ± 0.1	4861.48 ± 0.11	0.57 ± 0.08	5.3 ± 0.1
2009.27 ± 0.11	1.90 ± 0.11	6.1 ± 0.1	5048.89 ± 0.11	0.30 ± 0.03	5.4 ± 0.1
2083.84 ± 0.13	0.14 ± 0.06	7.3 ± 0.2 [b]	5237.57 ± 0.13	0.52 ± 0.04	5.0 ± 0.1
2169.1 ± 0.3	~0	···	5491.67 ± 0.19	0.72 ± 0.06	4.7 ± 0.1
2210.53 ± 0.15	0.45 ± 0.13	6.7 ± 0.1 [b]	5496.18 ± 0.23	0.75 ± 0.07	4.7 ± 0.1
2264.81 ± 0.15	~0	···	5665.40 ± 0.08	0.40 ± 0.18	4.8 ± 0.2
2285.71 ± 0.05	1.51 ± 0.16	6.1 ± 0.1	5759.6 ± 0.3	0.53 ± 0.10	4.6 ± 0.1
2609.43 ± 0.09	~0	···	5859.73 ± 0.12	1.11 ± 0.09	4.1 ± 0.1
2664.81 ± 0.07	0.42 ± 0.16	6.5 ± 0.2	5920.23 ± 0.08	1.49 ± 0.11	3.9 ± 0.1
2745.21 ± 0.16	~0	···	5965.36 ± 0.18	1.37 ± 0.11	3.9 ± 0.1
2814.85 ± 0.16	2.18 ± 0.14	5.8 ± 0.1	6070.40 ± 0.19	0.30 ± 0.02	4.5 ± 0.1
2855.90 ± 0.07	21.4 ± 0.8	4.8 ± 0.1	6260.0 ± 0.4	0.31 ± 0.09	4.2 ± 0.1
3001.95 ± 0.23	4.28 ± 0.22	5.4 ± 0.1	6572.10 ± 0.19	0.51 ± 0.04	3.5 ± 0.1
3063.29 ± 0.12	2.60 ± 0.12	5.6 ± 0.1	6725.45 ± 0.19	1.40 ± 0.14	2.8 ± 0.1

[a] Value adopted from Ref. 15. Total of β branching includes delayed neutron emission probability of $(2.6 \pm 0.5)\%$ from Ref. 29. Q_β of 7.51 ± 0.05 MeV adopted from this work.

[b] $\log f_1 t > 8.5$, so cannot exclude first-forbidden unique β transition.

C. Levels of ^{93}Rb

Again no reaction studies of the ^{93}Rb level structure have been reported. As a result, the proposed spin and parity assignments are based on the proposed decay scheme as well as the reported multipolarity of the five most intense γ-ray transitions. The first excited state at 253.3 keV has been reported to be depopulated by an $M1$ transition[15] which limits the spin to $\frac{3}{2}^-$, $\frac{5}{2}^-$, or $\frac{7}{2}^-$. β feeding to this level with a logft value of 6.5 also limits the spin-parity to $\frac{1}{2}^\pm$, $\frac{3}{2}^\pm$, or $\frac{5}{2}^-$. Based on these two arguments the spin-parity possibilities for this level are $\frac{3}{2}^-$ and $\frac{5}{2}^-$. The $\frac{3}{2}^-$ possibility is preferred from the systematics of odd-A rubidium isotopes, where the lighter isotopes have a ground-state J^π of $\frac{3}{2}^-$, indicating the presence of a low-lying level in ^{93}Rb with this same spin and parity. Such a state would result from a $2p_{3/2}$ proton hole.

The 266.8-keV level is depopulated by a ground-state transition having an $E2$ multipolarity and is fed in β decay with a logft value of 6.1. This suggests spin and parity possibilities of $\frac{1}{2}^-, \frac{3}{2}^-$. The former is preferred since it could result from promoting the odd proton to the $2p_{1/2}$ orbit.

The 324.0-keV level is depopulated by an $M1$ multipolarity ground-state transition and is fed in β decay with a logft value of 5.9. As a result, the only value possible for the spin and parity is $\frac{3}{2}^-$. Finally, the level at 506.0 keV is depopulated by two $M1$ transitions and fed in β decay with a logft value of 5.9. Thus the spin-parity possibilities are limited to $\frac{1}{2}^-$ or $\frac{3}{2}^-$.

Only the ground state and third excited state can be limited to a single spin-parity possibility. Therefore only those γ-ray transitions which feed these levels provide useful limitations on the spin-parity possibilities of the levels they depopulated. These arguments would be redundant so they will only be quoted for each group of levels. The levels with possible spin-parity values of

TABLE VIII. Comparison of γ-ray intensities with other ^{93}Kr studies.

Energy	This work	Achterberg *et al.* (Ref. 15)	Brissot[a] *et al.* (Ref. 17)
70.57	64 ± 3	110 ± 40	
182.02	232 ± 12	223 ± 15	240
252.51	810 ± 40	1000 ± 100	1850
253.42	1700 ± 90	1505 ± 150	660
266.83	850 ± 40	855 ± 40	820
323.89	1000 ± 50	1000 ± 50	1000
496.56	75 ± 4	61 ± 5	86
820.45	154 ± 8	135 ± 10	180
1026.19	90 ± 5	62 ± 7	83
1214.98	73 ± 4	58 ± 7	
1296.08	78 ± 4	45 ± 4	84
1387.92	56 ± 4		83
1505.76	93 ± 5	64 ± 7	73
1596.20	57 ± 3		
1627.10	82 ± 4	56 ± 8	73
1641.08	60 ± 3	61 ± 7	58
1697.84	58 ± 3		43
1742.49	53 ± 3	32 ± 5	51
1961.83	74 ± 4	41 ± 5	56
2018.87	58 ± 3	27 ± 4	54
2035.36	75 ± 4	51 ± 7	59
2349.96	306 ± 16	164 ± 21	239
2496.05	95 ± 5	56 ± 10	69
2602.61	174 ± 9	104 ± 10	154
2855.95	90 ± 5	45 ± 10	76

[a]The intensity uncertainties are reported to vary between 5 and 10% depending on the γ-ray intensity value.

$(\frac{1}{2}^-, \frac{3}{2}^\pm, \frac{5}{2}^-)$ are fed in β decay with $\log f_1 t$ values greater than 8.5 and depopulated by a ground-state transition. If the $\log f_1 t$ values are less than 8.5, the spin-parity values possible would be $(\frac{1}{2}^-, \frac{3}{2}^\pm)$. Another group of levels has a possible spin-parity assignment of $(\frac{1}{2}^+, \frac{3}{2}^+)$ based on β feeding with $\log ft$ values less than 5.9. Only the level at 2855.9 keV can be limited to a single spin-parity assignment of $\frac{3}{2}^+$ on the basis of β feeding with a $\log ft$ value less than 5.9 and depopulation by a ground-state γ-ray transition.

The only single-particle states which appear to be observed are the ground state and the first two excited states. The other low-lying states generally have negative parity and probably result from coupling these single-particle states to the excitations of the even neutron configuration.

In conclusion, although the decay schemes presented in this work contain great detail concerning the β and γ transitions, the firm assignment of spins and parities to the levels awaits detailed internal conversion and angular correlation measurements. Confirmation of the suggested ^{93}Rb ground-state spin by direct measurement (e.g., by laser beam techniques) would aid greatly in extending the level interpretations sketched briefly. Equally pressing is the need to remeasure the ground-state β branches in order to use these decay transitions in confirming the postulated ground-state spin-parity assignments. A program on this measurement, as part of a more extensive survey, is now underway at this laboratory.

†Prepared for the U. S. Energy Research and Development Administration under Contract No. W-7405-eng-82.

*Present address: Radiation Research Laboratory, University of Iowa, Iowa City, Iowa 52240.

[1]W. L. Talbert, Jr., and R. J. Hanson, Phys. Rev. C 8, 1945 (1973).

[2]S. A. E. Johansson, Nucl. Phys. 64, 147 (1965).

[3]E. Cheifetz, R. C. Jared, S. G. Thompson, and J. B. Wilhelmy, Phys. Rev. C 5, 2041 (1972).

[4]E. Achterberg, F. C. Igesias, A. E. Jech, J. A. Moragues, D. Otero, M. L. Perez, A. N. Proto, J. J Rossi, W. Scheuer, and J. F. Suarez, Phys. Rev. C 7, 365 (1973).

[5]F. K. Wohn, W. L. Talbert, Jr., R. S. Weinbeck, M. D. Glascock, and J. K. Halbig, Phys. Rev. C 11, 1455 (1975).

[6]C. Lieber, Naturwiss 27, 421 (1939).

[7]K. Fritze and T. J. Kennett, Can. J. Phys. 38, 1614 (1960).

[8]C. R. Dillard, R. M. Adams, H. Finston, and A. Turkevich, *The Fission Products* (National Nuclear Energy Series, Division IV, 1951).

[9]G. H. Carlson, W. C. Schick, Jr., W. L. Talbert, Jr., and F. K. Wohn, Nucl. Phys. A125, 267 (1969).

[10]J. R. Clifford, W. L. Talbert, Jr., F. K. Wohn, J. P. Adams, and J. R. McConnell, Phys. Rev. C 7, 2535 (1973).

[11]H. Bakhru and S. K. Mukherjee, Nucl. Phys. 61, 56 (1965).

[12]W. Herzog and W. Grimm, Z. Phys. 257, 424 (1972).

[13]P. Cavallini, F. Schussler, and A. Moussa, C. R. Acad. Sci. 272, 394 (1971).

[14]B. M. Preedom, E. Newman, and J. C. Hiebert, Phys. Rev. 166, 1156 (1967).

[15]E. Achterberg, F. C. Iglesias, A. E. Jech, J. A. Moragues, D. Otero, M. L. Perez, A. N. Proto, J. J. Rossi, and W. Scheuer, Phys. Rev. C 10, 2526 (1974).

[16]V. R. Casella, J. D. Knight, and R. A. Naumann, Nucl. Phys. A239, 83 (1975).

[17]R. Brissot, F. Schussler, E. Monnand, and A. Moussa, Nucl. Phys. A238, 149 (1975).

[18]J. R. McConnell and W. L. Talbert, Jr., Nucl. Instrum. Methods 128, 227 (1975).

[19]W. C. Schick, Jr., USAEC Report No. IS-3460, 1975 (unpublished).

[20]R. C. Greenwood, R. G. Helmer, and R. J. Gehrke, Nucl. Instrum. Methods 77, 141 (1970).

[21]R. G. Helmer, R. C. Greenwood, and R. J. Gehrke,

Nucl. Instrum. Methods 96, 1973 (1971).
[22]R. C. Greenwood, R. G. Helmer, and R. J. Gehrke (private communication).
[23]L. Multhauf and K. G. Tirsell (private communication).
[24]R. Gunnink, J. B. Niday, R. P. Anderson, and R. A. Meyer, USAEC Report No. UCID-15439, 1969 (unpublished).
[25]D. C. Camp and G. L. Meredith, Nucl. Phys. A166, 349 (1971).
[26]G. Aubin, J. Barrette, M. Barrette, and S. Monaro, Nucl. Instrum. Methods 76, 93 (1969).
[27]W. F. Edwards, F. Boehm, J. Rogers, and E. J. Seppi, Nucl. Phys. 63, 97 (1965).
[28]C. J. Bischof, Ph.D. thesis, Iowa State University, 1975 (unpublished).
[29]W. L. Talbert, Jr., A. B. Tucker, and G. M. Day, Phys. Rev. 177, 1805 (1969).
[30]M. D. Glascock, W. L. Talbert, Jr., and C. L. Duke, Phys. Rev. C 13, 1630 (1976).
[31]S. Raman and N. B. Gove, Phys. Rev. C 7, 1995 (1973).
[32]D. J. Horen and W. B. Ewbank, *Nuclear Level Schemes* $A = 45$ *through* $A = 257$ *from Nuclear Data Sheets* (Academic, New York, 1973).
[33]R. Muller, Ph.D. thesis, Technischen Universität, München, 1973 (unpublished).
[34]E. A. Henry, W. L. Talbert, Jr., and J. R. McConnell, Phys. Rev. C 7, 222 (1973).
[35]L. R. Medsker, Nucl. Data Sheets 10, 1 (1973).
[36]L. R. Medsker, Nucl. Data Sheets 12, 431 (1974).
[37]M. I. Macias-Marques, Ph.D. thesis, Centre de Orsay, Université Paris-Sud, 1971 (unpublished), Orsay Report Series A, No. 843.
[38]J. Vervier, Nucl. Phys. 75, 17 (1966).
[39]D. C. Kocher, Nucl. Data B8, 527 (1972).